SUPPORTING INFORMATION

A comparative analysis of synthetic quorum sensing modulators in *Pseudomonas aeruginosa*: New insights into mechanism, active efflux susceptibility, phenotypic response, and next-generation ligand design

Joseph D. Moore,[1] Francis M. Rossi,[2] Michael A. Welsh,[1] Kayleigh E. Nyffeler,[1] and Helen E. Blackwell[1,*]

[1]*Department of Chemistry, University of Wisconsin–Madison, 1101 University Ave., Madison, WI 53706, USA;* [2]*Department of Chemistry, SUNY Cortland, Cortland, NY 13045, USA*

CONTENTS.

* To whom correspondence should be addressed: blackwell@chem.wisc.edu

Table S1*:* Bacterial strains and plasmids used in this study.

Strain or plasmid	Relevant properties[a]	Ref.
Strains		
P. aeruginosa		
PAO1	Wild-type, isolated by B. Holloway from human wound	1
PAO-JP2	PAO1 *lasI*::Tet *rhlI*::Tn501-2; Hg^R Tc^R	2
PAO-JG21	PAO-JP2 Δ(*mexA-mexB-oprM*)	3
E. coli		
JLD271	K-12 Δ*lacX74 sdiA271*::Cam; Cl^R	4
S17-1::λpir	Mobilizer strain	5
Plasmids		
p*lasI*-LVA*gfp*	*lasI'-gfp*[LVA] transcriptional fusion; Cb^R	6
pSC11	Broad host range *lasI'-lacZ* reporter; Ap^R	7
pJN105L	Arabinose-inducible expression vector for *lasR*; pBBRMCS backbone; Gm^R	8

[a] Abbreviations: Hg^R, mercury resistance; Tc^R, tetracycline resistance; Cl^R, chloramphenicol resistance; Cb^R, carbenicillin resistance; Ap^R, Ampicillin resistance; Gm^R, gentamicin resistance.

Note S1: Extended rationale for compound selection.

The structures of the LasR modulator library members are shown in Figure 2 in the main text. The Group A sub-class of our LasR modulator library comprises compounds that retain the homoserine lactone head group functionality, yet have modifications within the acyl tail region. This class of AHLs has historical significance, as it has been a primary focus of much early research focused toward identifying small-molecule modulators of LuxR-type receptors.[9,10] AHLs **2**–**6** were either discovered or designed to be active in a variety of LuxR-type receptors and elicit a basal level of activity against LasR to which other compounds could be compared. *N*-(3-oxo-octanoyl)-L-homoserine lactone (**2**; OOHL) and *N*-(3-oxo-hexanoyl)-L-homoserine lactone (**3**; OHHL) are common, naturally occurring AHLs that are not native to *P. aeruginosa*.[11] AHLs **4**–**6** were chosen due to their effective inhibition of closely related LasR homologues: heptyl HL **4** was originally reported by the Winans laboratory in 1998 to be an inhibitor of the *Agrobacterium tumefaciens* LuxR-type receptor TraR,[12] and aryl HLs **5** and **6** were reported by Doutheau and co-workers in 2002 to be inhibitors of the *Vibrio fischeri* receptor LuxR.[13] Each of these compounds was later shown to possess antagonistic activity toward LasR.[14]

Since these early reports, many subsequent studies have focused on the identification of compounds that specifically target LasR within the *P. aeruginosa* QS network, and the remainder of the compounds selected for our library constitute some of the most active LasR modulators from these studies. Non-native aryl HLs **7**–**9** were developed by our laboratory, with **7** and **8** representing two of our most potent LasR antagonists and **9** representing a potent LasR agonist.[15,16] Aryl HL **10** ("chlorolactone"; CL) was initially reported by the Bassler laboratory as an inhibitor of the QS receptors CviR in *Chromobacterium violaceum* and LuxN in *Vibrio harveyi*;[17,18] more recently, Bassler and coworkers demonstrated that **10** is also an inhibitor of the *P. aeruginosa* LasR and RhlR receptors.[19] The final AHL in Group A, the isothiocyanate-functionalized AHL **11** (ITC-12), is a LasR partial agonist (originally designed as an irreversible LasR inhibitor) developed by Meijler and coworkers.[20] AHL **11**, a close analog of the native LasR ligand, OdDHL, has been shown to inhibit both biofilm formation and pyocyanin production in wild-type *P. aeruginosa* PAO1 and is believed to act via covalent modification of the Cys-79 residue in the LasR ligand-binding site.

Complementary to the Group A compounds, several research groups have reported LasR modulators that have alternative AHL head groups yet retain the 3-oxo-C12 acyl tail. Compounds **12**–**15**, which constitute Group B, are outstanding compounds of this class. Aryl head group compounds **12**, **13**, and **14** were the most active LasR antagonists developed in focused studies by our laboratory,[21] the Spring laboratory,[22] and the Suga laboratory,[23] respectively. The other compound included in Group B, cyclohexanone derivative **15**, was also developed by the Suga laboratory and showed a moderate ability to partially agonize LasR.[24] We incorporated **15** into our studies because it is one of the few synthetic QS modulators that are commercially available (in addition to compounds **4**, **21**, and the naturally occurring AHLs included herein; all sold by Sigma-Aldrich).

Group C comprises compounds that structurally mimic the native LasR ligand OdDHL but contain both non-natural head *and* acyl tail groups. The *meta*-bromothiolactone **16** (mBTL) was developed by the Bassler laboratory and was shown to act as a partial agonist (and partial antagonist) of both LasR and RhlR.[19] Despite this mixed activity profile, **16** was shown to inhibit virulence phenotypes in wild-type *P. aeruginosa* strain PA14, presumably in part by RhlR

agonism (as we recently demonstrated).[25] A cyclopentyl analog of OdDHL, **17** (C10-CPA), developed by the Kato laboratory, was shown to inhibit the activities of both LasR and RhlR in heterologous reporter strains; **17** was also found to inhibit production of pyocyanin, rhamnolipid, and elastase in the wild-type *P. aeruginosa* strain PAO1.[26] Greenberg and co-workers identified compound **18** (V-06-018) in a high-throughput screen for LasR inhibitors using a sizable corporate library.[27] Notably, this compound closely resembles aryl analog **12**, yet has the β-keto amide functionality inverted. Compound **18** was also found to inhibit pyocyanin and elastase production in PAO1.

The remaining compounds in the library (classified into Group D) show significant structural deviation from the canonical AHL-type autoinducers and have all been reported to exhibit LasR modulatory activity. Triphenyl derivatives **19** (TP-1), also identified by high-throughput screening by Greenberg and co-workers,[27] and **20** (TP-5), a TP-1 analog discovered through second-generation screening,[28] have been shown to directly modulate LasR activity in *P. aeruginosa* and *E. coli* LasR reporter strains. Compound **19** is an especially potent agonist of LasR; it is one of the few non-AHL-type compounds known with a reported EC_{50} value comparable to OdDHL. The interactions of **19** with LasR have been further characterized by X-ray crystallography by Zou and Nair;[29] their structure of the LasR ligand-binding domain complexed to **19** reveals this triphenyl ligand to bind in the same site as OdDHL. In contrast to **19**, triphenyl derivative **20** is a moderate antagonist of LasR. It could not be cocrystallized with the LasR ligand-binding domain due to the instability of the protein:**20** complex.[29] Such *in vitro* LuxR-type receptor destabilization has been previously observed for other small molecule antagonists, leading to the assertion that some antagonists may deactivate LuxR-type receptors primarily by destabilizing the receptor.[30]

Group D also includes bromofuranone **21** (C-30), which is a natural product derivative with QS-modulatory activity and is marketed by Sigma-Aldrich as such. Indeed, this compound is one of the most frequently cited synthetic small molecule modulators of LuxR/LuxI-type QS.[10] This compound was shown by the Givskov laboratory to inhibit the *las* system in LasR reporters harbored by wild-type *P. aeruginosa (*PAO1).[31] Phenotypic experiments showed that **21** decreased production of exoprotease, pyoverdine, and chitinase in PAO1 – all of which are under the control of the *las* system.[31] A reduction in LasR activity in wild-type *P. aeruginosa* was also observed when bromofuranone **21** was administered *in vivo* in mouse infection models.[32] We note that because all wild-type strains of *P. aeruginosa* contain fully functional autoinduction circuits, inhibition of any aspect of the circuit can manifest downstream inhibition of LasR. Though molecular modeling experiments have suggested that **21** interacts with the LasR ligand-binding pocket,[33,34] only very recently has **21** been reported to directly inhibit LasR in an *E. coli* reporter heterologously producing LasR.[35] Interestingly, microarray experiments by Givskov and co-workers showed that transcription of the *lasRI* genes was not significantly affected by addition of **21**. Since the *lasRI* genes are directly regulated by LasR, we believe this contradicts suggestions that **21** acts directly on LasR. Certainly, genes associated with QS regulation were significantly repressed,[31] but this may be due to interaction of **21** with another component of the *las* QS system. We included **21** in the current study to test these hypotheses and further clarify the mechanism by which this established QS modulator acts in *P. aeruginosa*. Lastly, compound **22** (PD-12) was identified as a LasR inhibitor by the Greenberg laboratory and, to our knowledge, has the strongest LasR-inhibitory potency reported for any small molecule to date (IC_{50} = 30 nM in the *P. aeruginosa ΔlasIrhlI* strain PAO-MW1).[27]

Table S2: Previously reported QS-modulatory activities for compounds used in this study.

Library compound	Receptor(s) targeted	Reporter type and assay results[a]	Phenotypic assay results	Pertinent Refs.
1 (OdDHL)	*P. aeruginosa* LasR	Agonist (native ligand)		
2 (OOHL)	*A. tumefaciens* TraR	Agonist (native ligand)		
3 (OHHL)	*V. fischeri* LuxR	Agonist (native ligand)		
4	LasR, TraR	LasR: *lasI-lacZ* – 15% inhibition at 5 μM TraR: *traI-lacZ* – >90% inhibition at 10 μM	None	[12,14]
5	LasR, LuxR	LasR: *lasI-lacZ* – 18% inhibition at 5 μM LuxR: *luxI-luxCDABE* – IC_{50} = 2 μM	None	[13,14]
6	LasR, LuxR	LuxR: *luxI-luxCDABE* – IC_{50} = 2 μM LasR: *lasI-lacZ* – 20% inhibition at 5 μM	None	[13,14]
7	LasR, LuxR, TraR	LasR: *lasI-lacZ* – IC_{50} = 6 μM LuxR: *luxI-luxCDABE* – IC_{50} = 4 μM TraR: *traI-lacZ* – IC_{50} = 6 μM	*P. aeruginosa* PAO1 pyocyanin – 10–30% inhibition at 50 μM PAO1 biofilm – 40% inhibition at 50 μM PAO1 elastase – 70% inhibition at 20 μM	[14,15,20,36]
8	LasR, LuxR, TraR	LasR: *lasI-lacZ* – IC_{50} = 300 nM LuxR: *luxI-luxCDABE* – IC_{50} = 1 μM TraR: *traI-lacZ* – IC_{50} = 1 μM	PAO1 elastase – 40% inhibition at 20 μM	[14]
9	LasR, LuxR, TraR	LasR: *lasI-lacZ* – agonist; EC_{50} = 10 μM LuxR: *luxI-luxCDABE* – IC_{50} = 2 μM TraR: *traI-lacZ* – IC_{50} = 200 nM	None	[16]
10 (CL)	*C. violaceum* CviR, LasR, *V. harveyi* LuxN, *P. aeruginosa* RhlR	CviR: *vioA-gfp* – IC_{50} = 2 μM LasR: *rsaL-gfp* – 25% inhibition at 1 mM RhlR: *rhlA-gfp* – 50% inhibition at 1 mM	*P. aeruginosa* PA14 pyocyanin – no inhibition at 100 μM *V. harveyi* BB120 bioluminescence – IC_{50} = 40 μM	[17-19]
11 (ITC-12)	LasR	LasR: *lasI-lacZ* in PAO1 – IC_{50} = 100 μM LasR: *lasI-lacZ* in *E. coli* – IC_{50} = 30 μM	PAO1 pyocyanin – 40% inhibition at 50 μM PAO1 biofilm – 45% inhibition at 50 μM	[20]
12	LasR	LasR: *lasI-lacZ* – 55% inhibition at 10 μM *rsaL-yfp* in *P. aeruginosa*: – 30% inhibition at 10 μM	PAO1 pyocyanin – 70% inhibition at 50 μM	[21,36]
13	LasR	None	PAO1 pyocyanin – 75% inhibition at 50 μM; 93% inhibition at 200 μM PAO1 elastase – 63% inhibition at 200 μM	[22,36]
14	LasR, RhlR	LasR: *lasI-gfp*[LVA] in *P. aeruginosa* PAO-JP2 – 90% inhibition at 100 μM RhlR: *rhlI-gfp*[LVA] in PAO-JP2 – 70% inhibition at 10 μM	PAO-JP2 & PAO1 pyocyanin: no inhibition at 100 μM PAO-JP2 & PAO1 biofilm: qualitative increase at 50 μM (accompanied by change in morphology) PAO-JP2 (Δ*lasIrhlI*) elastase – 40% inhibition at 10 μM PAO1 elastase – 50% inhibition at 10 μM	[23]
15	LasR, RhlR	LasR: *lasI-gfp*[LVA] in PAO-JP2 – partial agonist; 45% activation at 400 μM; 40% inhibition at 100 μM	PAO-JP2 pyocyanin: 35% inhibition at 50 μM PAO1 pyocyanin: 70% inhibition at	[24]

		RhlR: *rhlI-gfp*[LVA] in PAO-JP2 – 70% inhibition at 50 μM	100 μM PAO-JP2 & PAO1 biofilm: qualitative decrease at 50 μM (accompanied by change in morphology) PAO-JP2 elastase – 95% inhibition at 100 μM PAO1 elastase – 95% inhibition at 100 μM	
16 (mBTL)	LasR, RhlR	LasR: *rsaL-gfp* – partial agonist; ~75% activation at 100 nM RhlR: *rhlA-gfp* – partial agonist; ~75% activation at 20 μM	PA14 pyocyanin – 80% at 100 μM PA14 in *C. elegans* fast-kill – 50% reduction in killing at 50 μM PA14 biofilm – 60% reduction in clogging time of flow chamber	[19]
17 (C10-CPA)	LasR, RhlR	LasR: *lasI-lacZ* in PAO1 – 90% inhibition at 250 μM RhlR: *rhlA-lacZ* in PAO1 – 80% inhibition at 250 μM	PAO1 rhamnolipid – 85% inhibition at 250 μM PAO1 pyocyanin – 50% inhibition at 50 μM PAO1 biofilm – qualitative inhibition at 250 μM PAO1 elastase – 75% inhibition at 250 μM	[26]
18 (V-06-018)	LasR	LasR: *rsaL-yfp* in *P. aeruginosa* MW1 – 75% max inhibition; IC_{50} = 10 μM	PAO1 pyocyanin – 90% inhibition at 100 μM PAO1 elastase – 60% inhibition at 100 μM	[27]
19 (TP-1)	LasR	LasR: *rsal-yfp* in PAO-MW1 – agonist; EC_{50} = 14 nM; LasR: *lasI-luxCDABE* in PAO-JP2 – agonist; EC_{50} = 40 nM	None	[28,37]
20 (TP-5)	LasR	LasR: *rsal-yfp* in PAO-MW1 – 90% max inhibition; IC_{50} = 50 μM	None	[28]
21 (C-30)	LasR, LuxR	LasR: *lasB-gfp*[ASV] in PAO1 – IC_{50} = 2 μM; in mouse – qualitative inhibition LasR: *lasB-gfp*[ASV] in *E. coli* MT102 – 90% inhibition at 100 μM **Note:** Many prior studies of **21** have shown its ability to inhibit LasR reporters, but the reporters utilized in these studies were most often harbored in *P. aeruginosa* strains containing an intact *lasRI* circuit. In those cases, it is possible that the inhibition of LasR activity may be due to upstream disruption of the QS autoinduction loop, especially given that **21** does significantly repress transcripts of genes coding for acyl carrier proteins involved in synthesis of QS autoinducers.[31] A recent assay showed inhibition of LasR in an *E. coli* reporter,[35] but **21** was dosed at concentrations that regularly induce cytotoxicity in our assays. LuxR: *luxI-gfp*[ASV] (*E. coli* biosensor in mouse) – qualitative repression	PAO1 mouse lung infection – at 0.25–2 μg/g body mass, increased survival time (~30%), 10–1000-fold increase in bacterial clearance, PAO1 biofilm – increased susceptibility to 100 μg/mL tobramycin at 10 μM C-30 PAO1 exoprotease – 80% inhibition at 10 μM PAO1 pyoverdine – >90% inhibition at 10 μM	[31,32,35,38]
22 (PD-12)	LasR	LasR: *rsaL-yfp* in PAO-MW1 – 80% max inhibition; IC_{50} = 30 nM	PAO1 pyocyanin – 40% inhibition at 10 μM (Greenberg); no inhibition at 50 μM (Spring) PAO1 elastase – 20% inhibition at 10 μM	[27,36]

[a]All assays were performed in a heterologous *E. coli* background unless otherwise noted.

Note S2: General considerations and conditions for whole-cell assays for compound activity on LasR.

Rationale. The following assays were adapted from literature sources (see protocols below) and significantly optimized for 96-well microtiter plates to provide the greatest dynamic range between positive and negative controls.

Preparation of bacterial strains. Freezer stocks of bacterial strains were maintained at -80 °C in Luria-Bertani (LB) medium and 20–50% glycerol. Bacterial overnight cultures were inoculated with single colonies (never exceeding 1 mm in diameter) that were isolated by streaking a freezer stock on an LB/agar (1.5%) plate with appropriate antibiotic supplements.

General assay conditions. Unless otherwise noted, bacteria were grown in a standard laboratory incubator at 37 ºC with shaking (200 rpm) in LB medium (autoclave-sterilized). All *P. aeruginosa* overnight cultures and subcultures were grown in Erlenmeyer flasks to maximize aeration. *P. aeruginosa* strain PAO-JP2 harboring p*lasI*-LVA*gfp* was grown in the presence of 200 μg/mL carbenicillin. The *P. aeruginosa* Δ(*mexAB-oprM)* strain PAO-JG21 was more sensitive to antibiotic selection and thus was grown in the presence of 50 μg/mL carbenicillin. All *E. coli* overnight cultures were grown in 13 mm x 100 mm test tubes. All *E. coli* subcultures were grown in Erlenmeyer flasks. *E. coli* strain JLD271 harboring plasmids pSC11 and pJN105L was grown in the presence of 100 μg/mL ampicillin and 10 μg/mL gentamicin. To minimize growth effects in 96-well plates, the following precautions were taken: (i) To reduce media evaporation, plates were incubated in stacks with "dummy plates" (containing sterile water in all wells) positioned on the top and bottom. Stacks of plates were placed in plastic containers to reduce air circulation. (ii) To reduce variation in ambient temperature, plates (including "dummy plates") were never stacked higher than six-fold.

Full protocols for reporter assays are described below. The full protocol for measuring elastase B activity in *P. aeruginosa* PAO1 is described in the Experimental Section of the main text.

Note S3: Full *P. aeruginosa* LasR reporter assay protocol.

To evaluate the modulatory activities of the library compounds on LasR in *P. aeruginosa*, strains PAO-JP2 or PAO-JG21 harboring the plasmid p*lasI*-LVA*gfp* were grown for 20 h. An appropriate amount of test compound stock solution (or OdDHL stock solution, as a control) in DMSO was added to the wells of black, clear-bottom 96-well microtiter plates (Costar 3904), with final DMSO concentrations not exceeding 1%. The overnight *P. aeruginosa* culture was diluted 1:100 in fresh LB medium (with no additional antibiotic supplement) and grown to an optical density at 600 nM (OD_{600}) of 0.3. For agonism assays, the subculture was dispensed in 200-μL portions into each compound-treated well of the microtiter plate. For antagonism assays, the subculture was pretreated with OdDHL (150 nM in PAO-JP2 or 20 nM in PAO-JG21) by adding the appropriate amount of an OdDHL stock solution in DMSO. The subculture was then dispensed in 200-μL portions into each compound-treated well of the microtiter plate. Subculture containing 1% DMSO and no added OdDHL was used as a control to mimic fully inhibited LasR.

Plates were incubated in a static laboratory incubator at 37 ºC for 6 h, and GFP production was detected using a Biotek Synergy 2 plate reader (Excitation: 500 nm, Emission: 540 nm). The final OD_{600} of each well was measured to normalize GFP production to cell density. In all assays, fluorescence readings were background-corrected relative to wells of LasR reporter subculture containing only 1% DMSO (no added compound). In agonism assays, the OD-normalized fluorescence of each compound was reported relative to the OD-normalized fluorescence of a well containing enough OdDHL to fully activate LasR. In antagonism assays, percent activity was calculated by normalizing background-corrected fluorescence to the control wells containing subculture treated with only OdDHL at its EC_{50} value. All synthetic compounds were tested in triplicate, and ≥ 3 separate trials were performed using unique cultures.

Note S4: Full *E. coli* LasR reporter assay protocol.

To evaluate the modulatory activities of library compounds on LasR heterologously expressed in *E. coli*, the strain JLD271[4] harboring plasmids pSC11 and pJN105L was grown overnight. The overnight culture was diluted 1:10 in fresh LB medium supplemented with 100 μg/mL ampicillin and 10 μg/mL gentamicin. The subculture was grown to an OD_{600} of 0.450, and arabinose was added to a final concentration of 4 mg/mL to induce LasR expression from the plasmid pJN105L. DMSO stock solutions of test compounds and *E. coli* subculture were added to clear 96-well microtiter plates (Costar 3370) as in the above *P. aeruginosa* reporter assays. The plates were incubated with shaking for 4 h.

The cultures were assayed for β-galactosidase activity following the Miller assay method, optimized for microtiter plates.[39] The OD_{600} of each well was recorded, and 50 μL aliquots from each well were transferred to the wells of a solvent-resistant 96-well microtiter plate (Costar 3879) containing 200 μL Z-buffer, 8 μL $CHCl_3$, and 4 μL 0.1% aqueous sodium dodecyl sulfate (SDS). Cells were lysed by aspirating and dispensing the mixtures 20 times with a 12-channel pipettor, after which the $CHCl_3$ was allowed to settle. A 150-μL aqueous aliquot from each well was transferred to a fresh clear-bottom 96-well microtiter plate. At t = 0 min, the assay was initiated by adding 25 μL of substrate, chlorophenol red-β-D-galactopyranoside (CPRG; 4 mg/mL in phosphate-buffered saline (PBS)), to each well. After development of the appropriate red color (~8 min), absorbance at 570 nm (A570) was measured for each well. Adjusted Miller Units were calculated using the following formula: $A570 \times (\text{Volume culture lysed in L})^{-1} \times (\text{Time CPRG incubated with lysate in min})^{-1} \times OD_{600}^{-1}$. Percent LasR activity for agonism and antagonism assays was calculated for each compound as in the above *P. aeruginosa* reporter assays. All synthetic compounds were tested in triplicate, and ≥ 3 separate trials were performed using unique cultures.

Table S3: LasR antagonism and agonism single-concentration assay data in the *P. aeruginosa* PAO-JP2 and *E. coli* JLD271 LasR reporter strains.

	P. aeruginosa PAO-JP2[a]				*E. coli* JLD271[b]			
	Agonism		Antagonism		Agonism		Antagonism	
Compound	Activity (%)[c]	SEM (%)	Inhibition (%)[d]	SEM (%)	Activity(%)[e]	SEM (%)	Inhibition (%)[f]	SEM (%)
1	88	6.8	-98	11.8	93	1.1	-79	13.9
2	21	6.6	50	8.5	61	5.4	-16	17.0
3	4	2.9	51	7.0	-4	3.4	73	5.5
4	-2	2.6	26	2.3	3	2.9	54	8.7
5	0	2.3	39	2.7	2	0.2	53	8.0
6	0	0.9	27	1.8	-1	0.2	55	10.6
7	-1	1.3	44	2.4	2	2.1	66	4.1
8	8	0.7	63	2.7	25	6.7	4	23.4
9	36	3.1	21	6.0	63	7.2	-53	15.1
10	3	0.8	60	2.8	11	0.9	14	20.8
11	119	17.7	-74	11.5	92	1.1	-72	11.2
12	8	5.8	65	3.0	30	3.0	-4	4.1
13	1	2.0	42	3.6	1	0.0	36	6.8
14	50	3.7	6	0.6	86	3.8	-66	8.4
15	7	2.0	32	13.9	89	3.0	-96	14.8
16	100	10.1	-85	7.7	88	8.1	-98	11.5
17	1	0.5	59	4.4	20	3.8	-36	16.3
18	3	2.5	83	1.7	2	0.7	46	6.8
19	104	25.8	-71	19.0	105	4.8	-112	11.1
20	0	2.3	79	2.6	0	0.0	12	12.5
21[g]	N/A	N/A	N/A	N/A	1	1.3	51	25.0
22	0	0.9	53	2.3	1	0.1	-1	3.8

[a] See Experimental Section and Table S1 for full assay and strain information. Compounds were screened at 100 μM. All screening data were background-corrected by subtracting the negative control (wells containing reporter strain + 2 μL DMSO only) from the experimental value. Percent (%) LasR activity was calculated by normalizing the background-corrected value to the fluorescence value obtained in wells containing reporter strain + OdDHL. Percent (%) LasR antagonism = 100% – % LasR activity). Negative antagonism values are indicative of agonism.
[b] See Experimental Section and Table S1 for full assay and strain information. Compounds were screened at 10 μM. All screening data were processed in the same manner as for the PAO-JP2/p*lasI*-LVA*gfp* screen.
[c] Assays performed in strain PAO-JP2/p*lasI*-LVA*gfp*. Percent agonism is given relative to 100 μM OdDHL.
[d] Assays performed in strain PAO-JP2/p*lasI*-LVA*gfp* in the presence of 150 nM OdDHL.
[e] Assays performed in strain JLD271/pJN105L/pSC11. Percent agonism is given relative to 10 μM OdDHL.
[f] Assays performed in strain JLD271/pJN105L/pSC11 in the presence of 2 nM OdDHL.
[g] Compound was cytotoxic to *P. aeruginosa* at 100 μM; data obtained in the *P. aeruginosa* LasR reporter were excluded from analysis.

Note S5: Rationale for exclusion of certain data points in dose–response curves.

As the compounds assayed in the current study vary widely in structure and, to some extent, in mechanism of action, we were careful to ensure that compounds were not acting via general growth inhibition or via nonspecific aggregation. Such off-target effects have plagued some past analyses of target compounds.[40,41] In Figure S5, we show the average final OD_{600} values at each test compound concentration for all compound dose–response assays in the *P. aeruginosa* PAO-JP2 and *E. coli* JLD271 LasR reporters. Any concentration of compound that elicited a statistically significant change in final OD_{600} (lower OD indicative of toxicity; higher OD indicative of compound aggregation/insolubility) was excluded from further analysis for determination of compound potency (i.e., EC_{50}/IC_{50} calculations).

Note S6: Comments on nonlinear regression parameters for sigmoidal fits.

We have previously shown (using a LasR reporter in *P. aeruginosa* strain PAO-JG21) that deletion of the active efflux pump MexAB-OprM affects the potency (i.e., concentration at which compounds are active) of pump-susceptible small molecule QS modulators, yet does not impact compound efficacy (maximum activity) or overall dose–response curve shape.[3] In the current study, we sought to perform accurate statistical analysis on the potency shift between the pump-active (PAO-JP2) and pump-mutant (PAO-JG21) strains for each compound to determine whether the shift was statistically significant. To do so, we chose to fit the dose–response curves in the PAO-JP2 and PAO-JG2 strains simultaneously for each compound, by applying global fitting to all parameters of the dose curve. We then applied shared constraints to all parameters other than the EC_{50} or IC_{50} values (i.e., sigmoid curve "top" and "bottom"; Hill slope). Next, using these globally fitted dose–response curves, we applied a t-test on the EC_{50}/IC_{50} values to determine if the potency shift was statistically significant. This t-test was performed based on the null hypothesis that all parameters of the sigmoidal curve were unchanged between pump-active and pump-mutant tests; the alternative hypothesis was that only the EC_{50}/IC_{50} values (not other parameters of the sigmoidal curve) were distinct.

We believe this method (as compared to fitting PAO-JP2 and PAO-JG21 dose response curves separately, then performing simple t-tests on the EC_{50}/IC_{50} values) is particularly powerful for analyzing dose curves such as those in Figure S1 (*e.g.*, compound **5**; see next page). We observe that the curve produced by dosing **5** into the PAO-JP2 LasR reporter does not effectively level off to a distinct "bottom" at the concentrations tested, but we can assume that the sigmoid bottom matches that of the PAO-JG21 dose curve. Consequently, we can still apply accurate statistical tests to these incomplete dose curves.

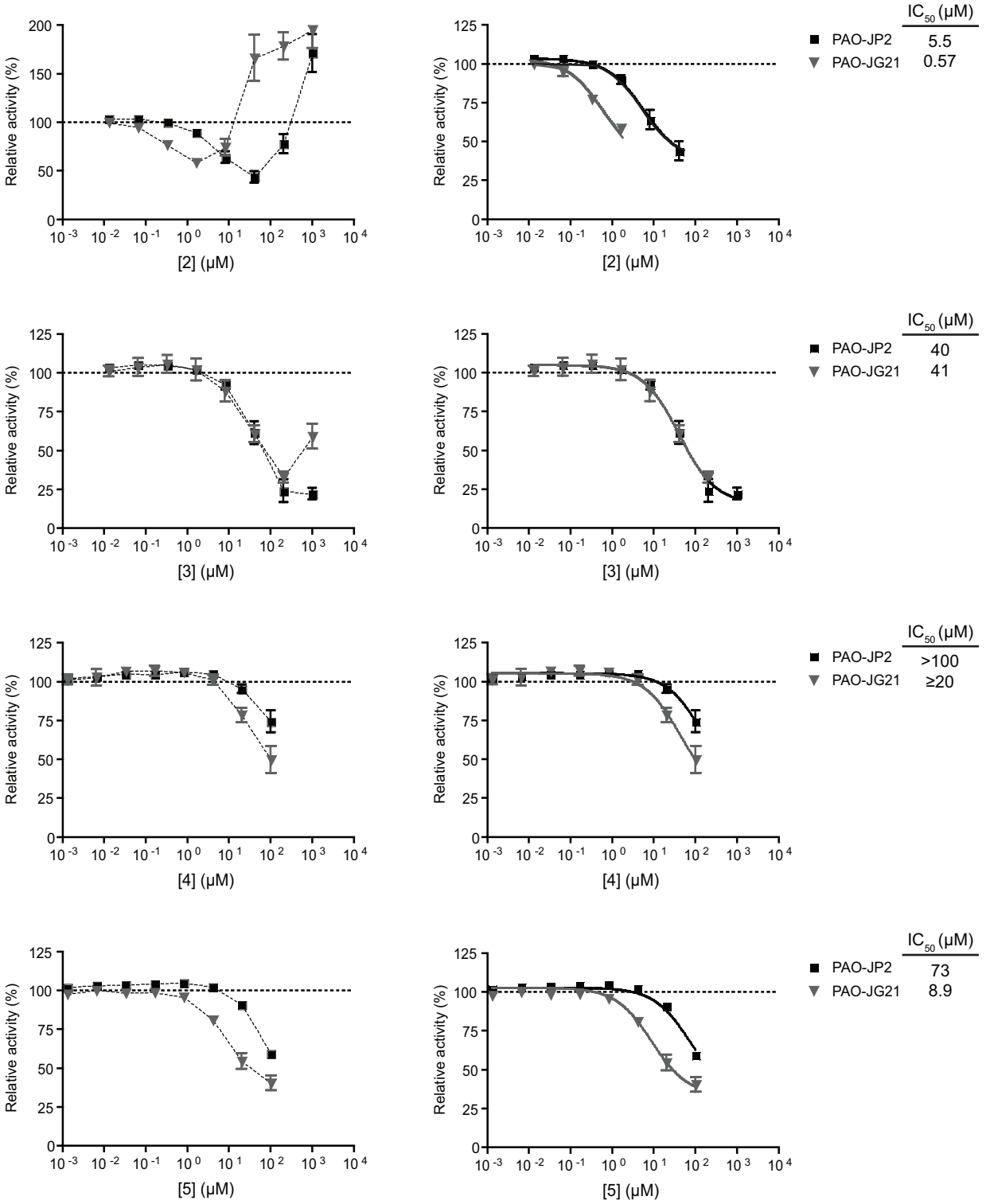

Figure S1*:* LasR antagonism dose responses and IC_{50} values for all tested compounds in the *P. aeruginosa* PAO-JP2 (black box) and PAO-JG21 (grey triangle) *lasI-gfp* reporter strains. Plots on left show the full dose–response including non-monotonic behavior, if applicable. Plots on right are truncated (if necessary) to show the dose–response curves of the concentration regime where LasR inhibition was observed. Compounds were screened against 150 nM OdDHL in PAO-JP2, and against 20 nM OdDHL in PAO-JG21. IC_{50} values were calculated from plots on right using GraphPad Prism. Error bars, SEM of n = 3 trials.

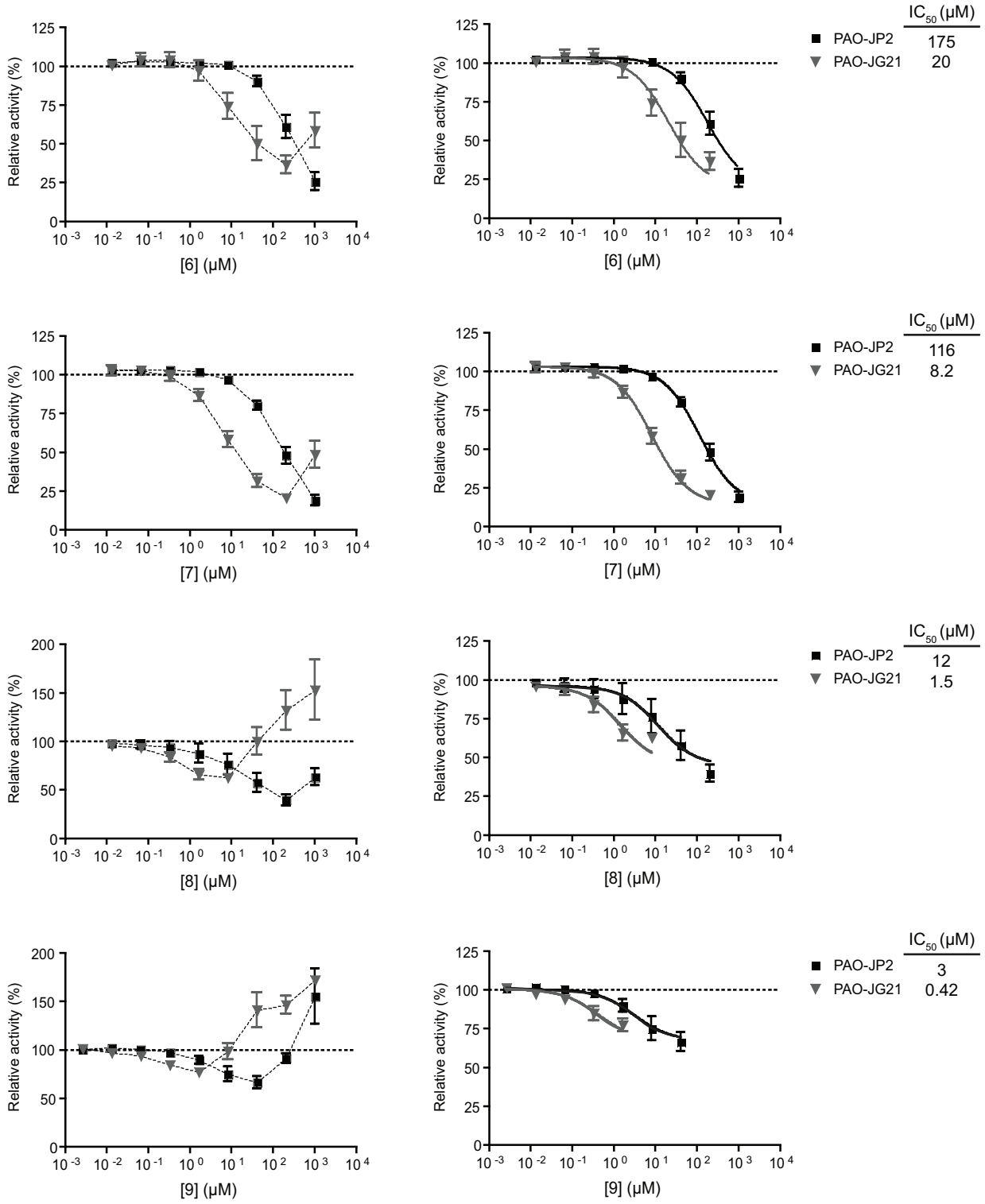

Figure S1 (continued): LasR antagonism dose responses and IC_{50} values for all tested compounds in the *P. aeruginosa* PAO-JP2 (black box) and PAO-JG21 (grey triangle) *lasI-gfp* reporter strains. Plots on left show the full dose–response including non-monotonic behavior, if applicable. Plots on right are truncated to show the dose–response curves of the concentration regime where LasR inhibition was observed. Compounds were screened against 150 nM OdDHL in PAO-JP2, and against 20 nM OdDHL in PAO-JG21. IC_{50} values were calculated from the plots on right using GraphPad Prism. Error bars, SEM of n = 3 trials.

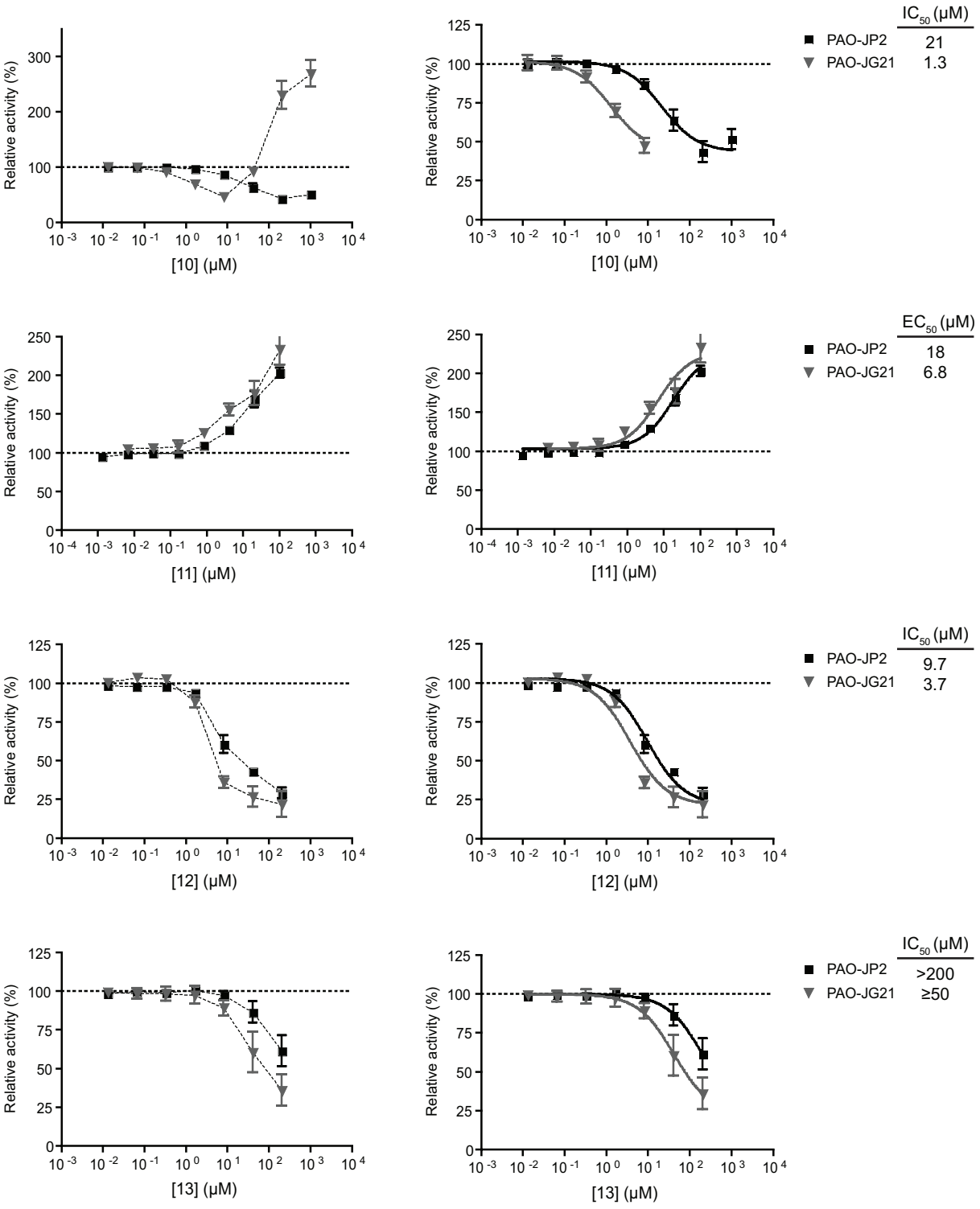

Figure S1 (continued): LasR antagonism dose responses and IC_{50} values (or EC_{50} values, for compounds that activated more strongly than OdDHL) for all tested compounds in the *P. aeruginosa* PAO-JP2 (black box) and PAO-JG21 (grey triangle) *lasI-gfp* reporter strains. Plots on left show the full dose–response including non-monotonic behavior, if applicable. Plots on right are truncated (if necessary) to show the dose–response curves of the concentration regime where LasR inhibition was observed. Compounds were screened against 150 nM OdDHL in PAO-JP2, and against 20 nM OdDHL in PAO-JG21. IC_{50} values and EC_{50} values were calculated from the plots on right using GraphPad Prism. Error bars, SEM of n = 3 trials.

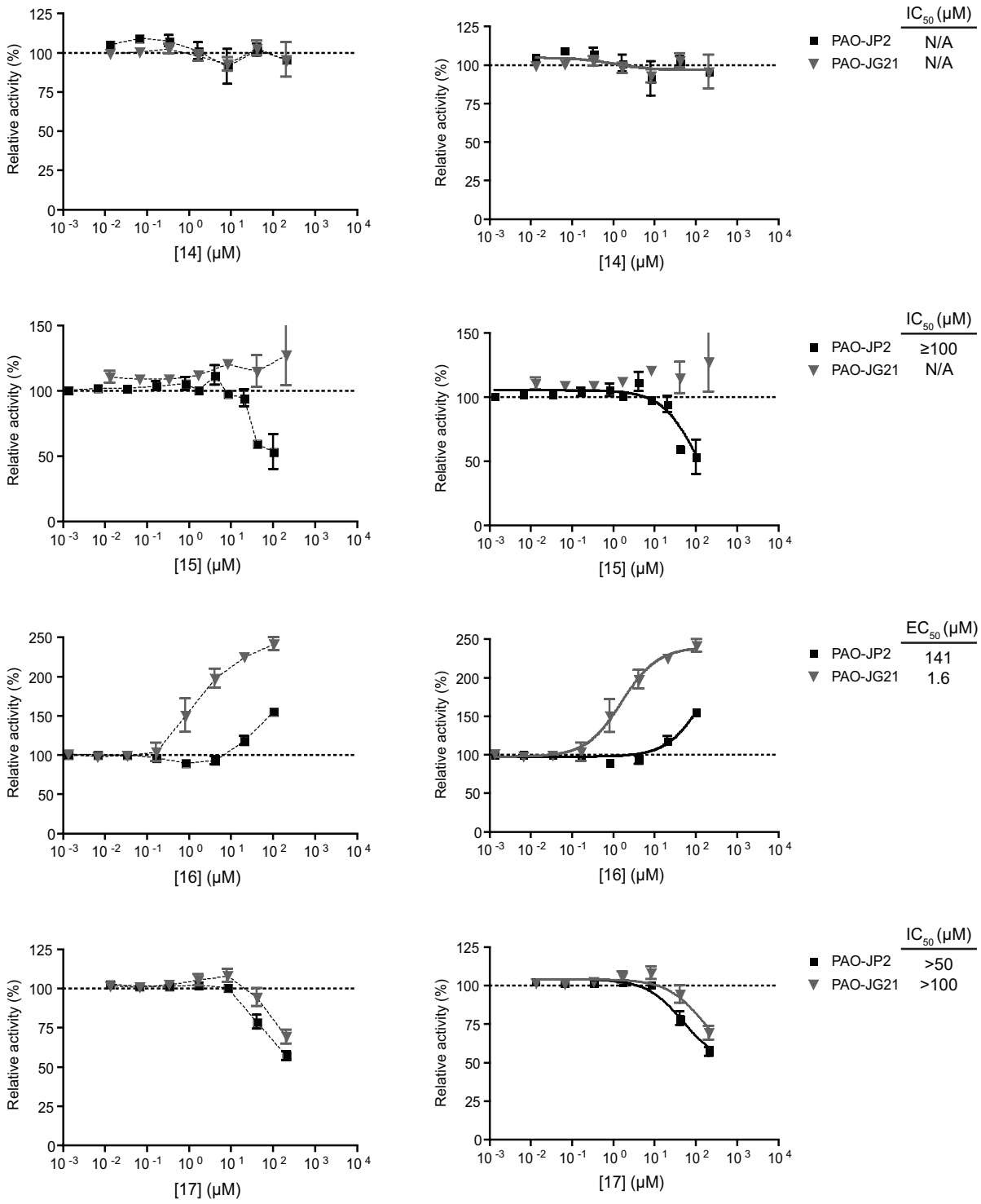

Figure S1 (continued): LasR antagonism dose responses and IC_{50} values (or EC_{50} values, for compounds that activated more strongly than OdDHL) for all tested compounds in the *P. aeruginosa* PAO-JP2 (black box) and PAO-JG21 (grey triangle) *lasI-gfp* reporter strains. Plots on left show the full dose–response. Plots on right are fitted to a sigmoidal curve. Compounds were screened against 150 nM OdDHL in PAO-JP2, and against 20 nM OdDHL in PAO-JG21. Where possible, IC_{50} values and EC_{50} values were calculated from the plots on right using GraphPad Prism. Error bars, SEM of n = 3 trials.

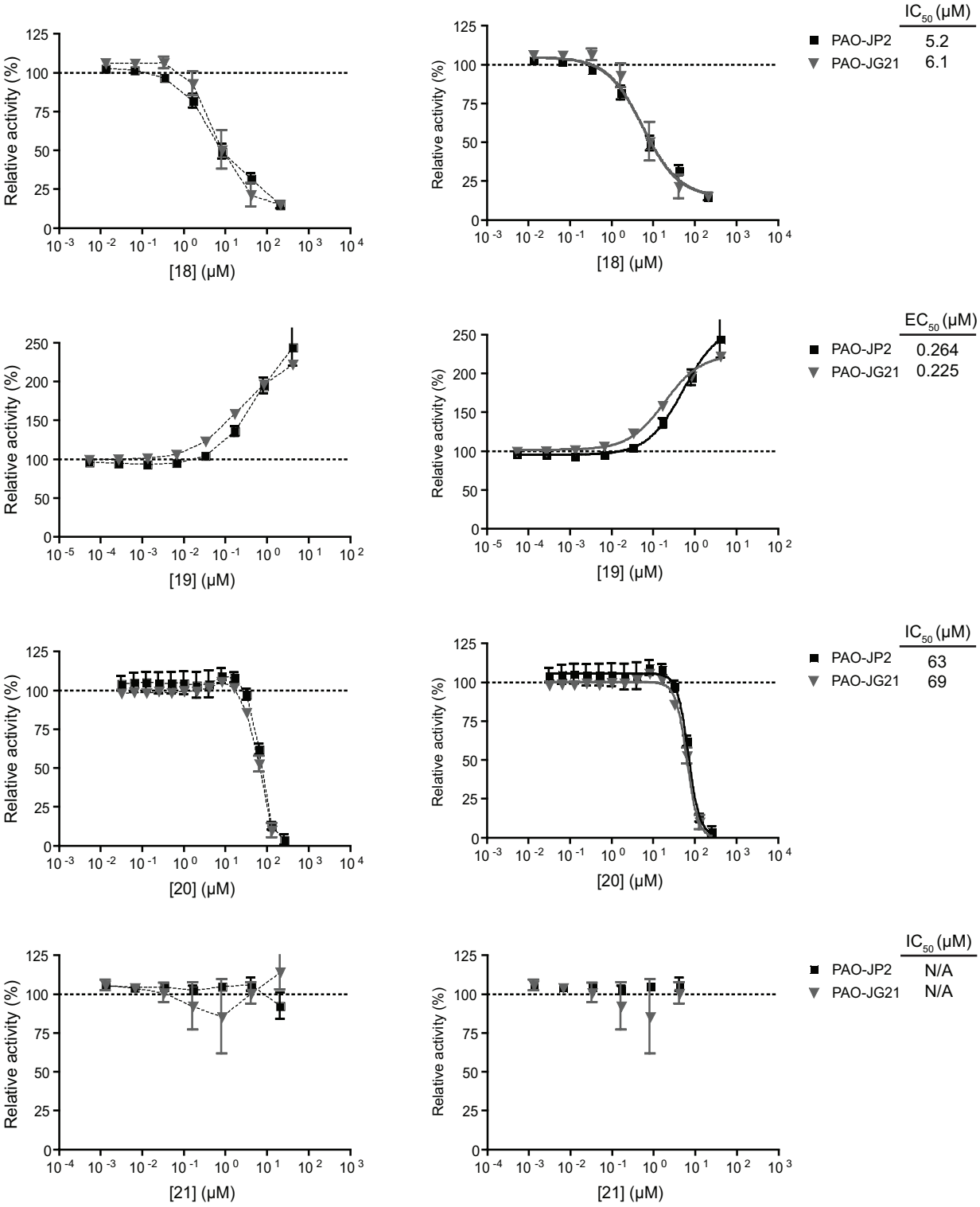

Figure S1 (continued): LasR antagonism dose responses and IC_{50} values (or EC_{50} values, for compounds that activated more strongly than OdDHL) for all tested compounds in the *P. aeruginosa* PAO-JP2 (black box) and PAO-JG21 (grey triangle) *lasI-gfp* reporter strains. Plots on left show the full dose–response. Plots on right are fitted to a sigmoidal curve. Compounds were screened against 150 nM OdDHL in PAO-JP2, and against 20 nM OdDHL in PAO-JG21. Where possible, IC_{50} values and EC_{50} values were calculated from the plots on right using GraphPad Prism. Error bars, SEM of n = 3 trials.

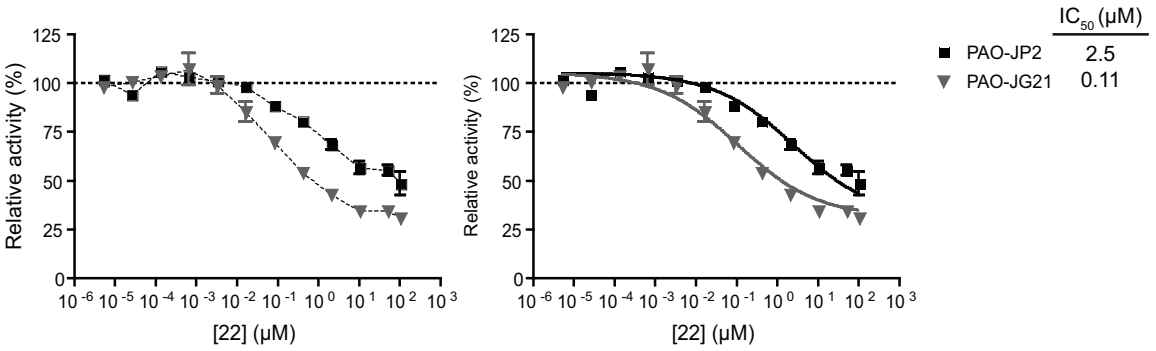

Figure S1 (continued): LasR antagonism dose responses and IC_{50} values for all tested compounds in the *P. aeruginosa* PAO-JP2 (black box) and PAO-JG21 (grey triangle) *lasI-gfp* reporter strains. The plots on left show the full dose–response. The plots on right are fitted to a sigmoidal curve. Compounds were screened against 150 nM OdDHL in PAO-JP2, and against 20 nM OdDHL in PAO-JG21. IC_{50} values were calculated from the plots on right using GraphPad Prism. Error bars, SEM of n = 3 trials.

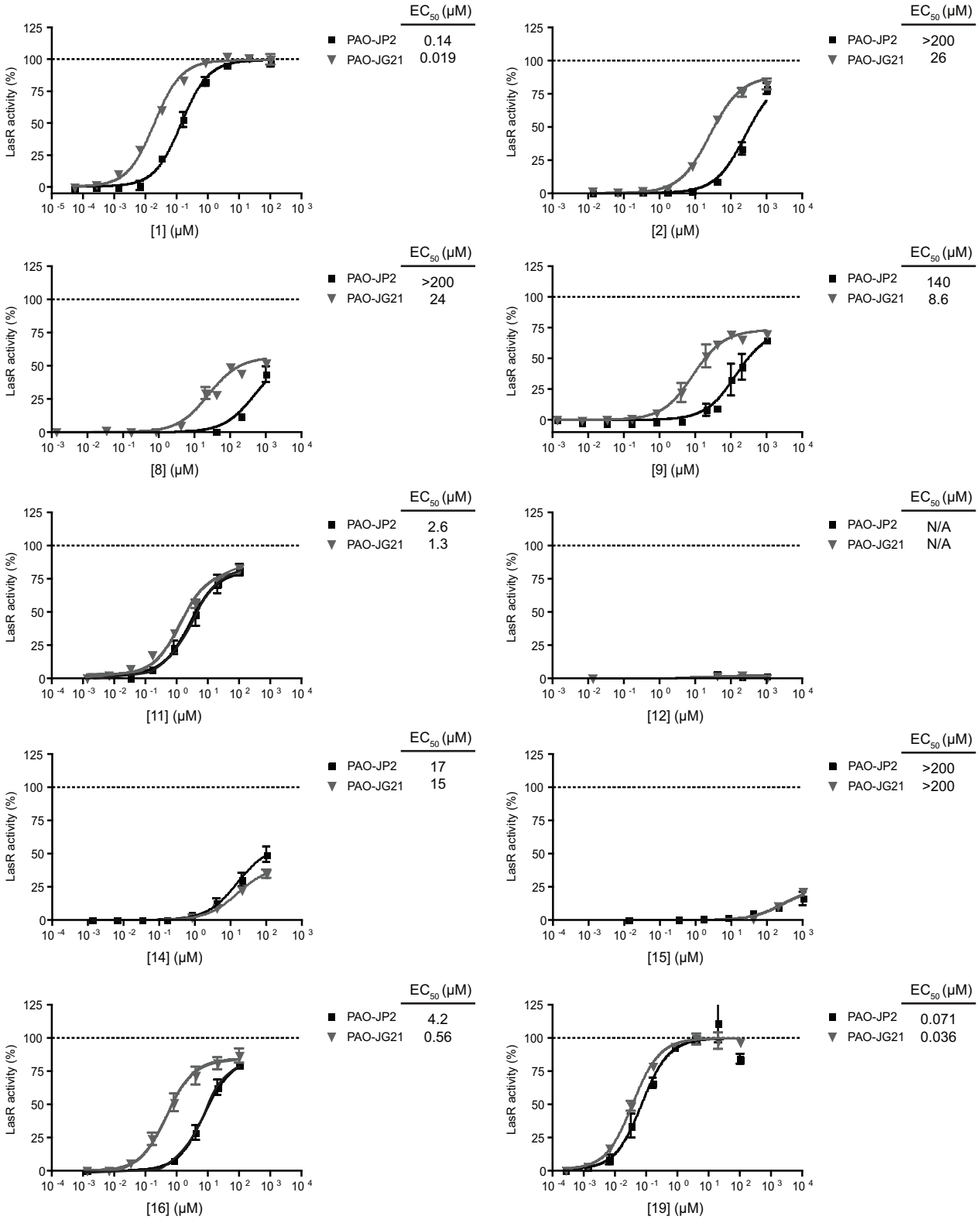

Figure S2*:* LasR agonism dose responses and EC_{50} values for all tested compounds in the *P. aeruginosa* PAO-JP2 (black box) and PAO-JG21 (grey triangle) *lasI-gfp* reporter strains. Where possible, EC_{50} values were calculated using GraphPad Prism. Error bars, SEM of n = 3 trials.

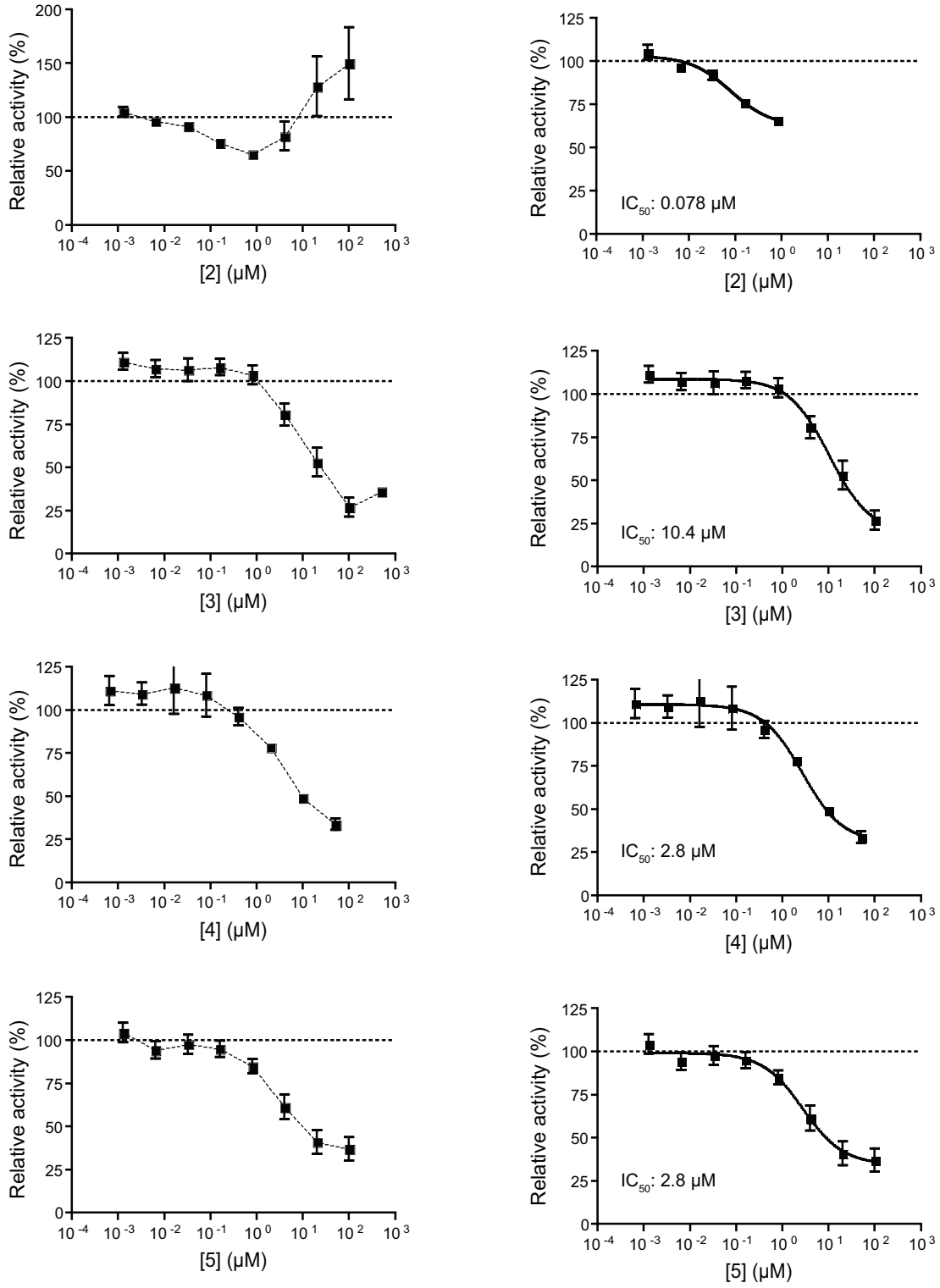

Figure S3*:* LasR antagonism dose responses and IC_{50} values for all tested compounds in the *E. coli* JLD271 *lasI-lacZ* reporter strain. Plots on left show the full dose–response including non-monotonic behavior, if applicable. Plots on right are truncated (if necessary) to show the dose–response curves of the concentration regime where LasR inhibition was observed. Compounds were screened against 2 nM OdDHL. IC_{50} values were calculated from the plots on right using GraphPad Prism. Error bars, SEM of n = 3 trials.

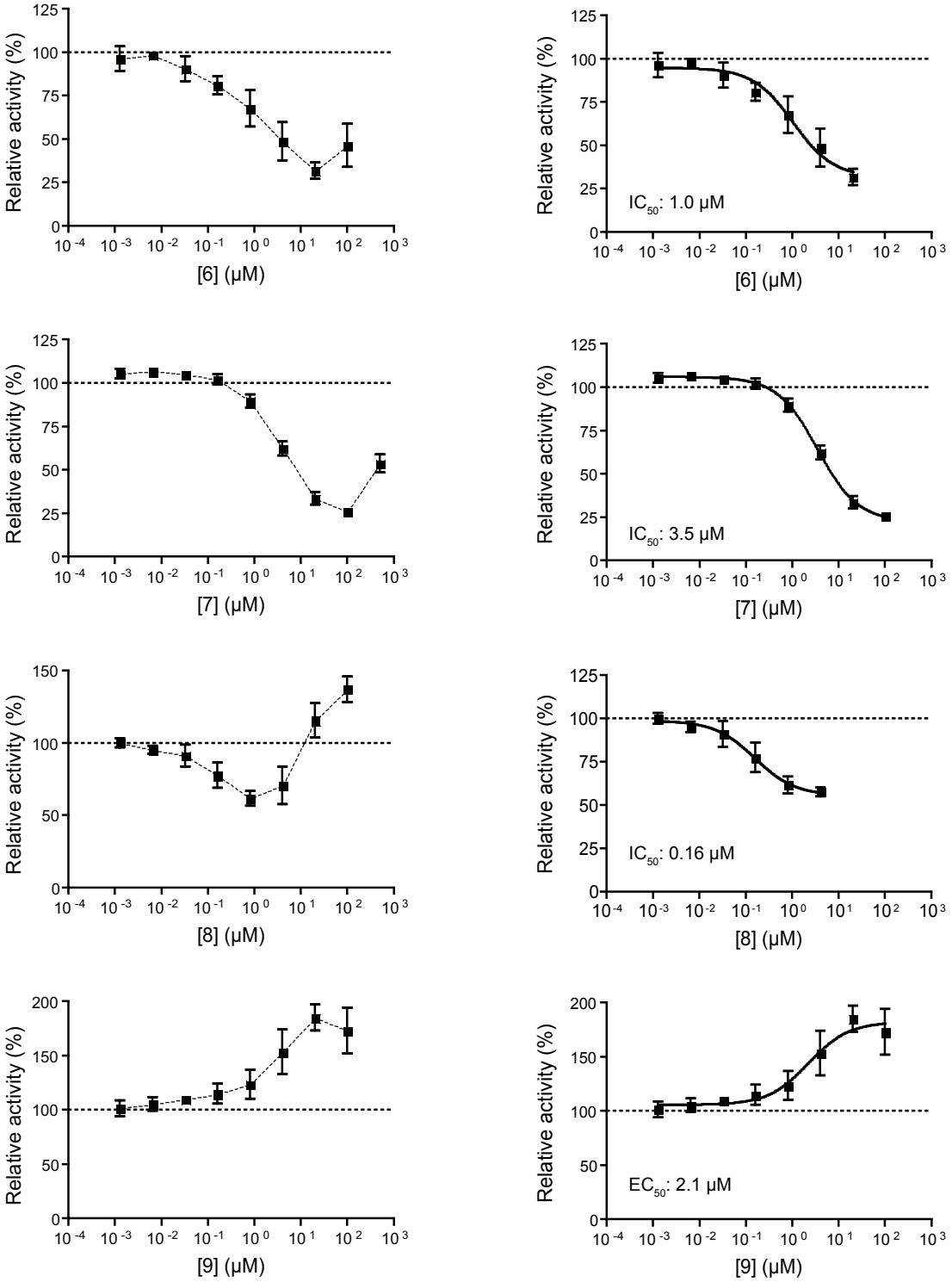

Figure S3 (continued): LasR antagonism dose responses and IC_{50} values (or EC_{50} values, for compounds that activated more strongly than OdDHL) for all tested compounds in the *E. coli* JLD271 *lasI-lacZ* reporter strain. Plots on left show the full dose–response including non-monotonic behavior, if applicable. Plots on right are truncated (if necessary) to show the dose–response curves of the concentration regime where LasR inhibition was observed. Compounds were screened against 2 nM OdDHL. IC_{50} values and the EC_{50} value were calculated from the plots on right using GraphPad Prism. Error bars, SEM of n = 3 trials.

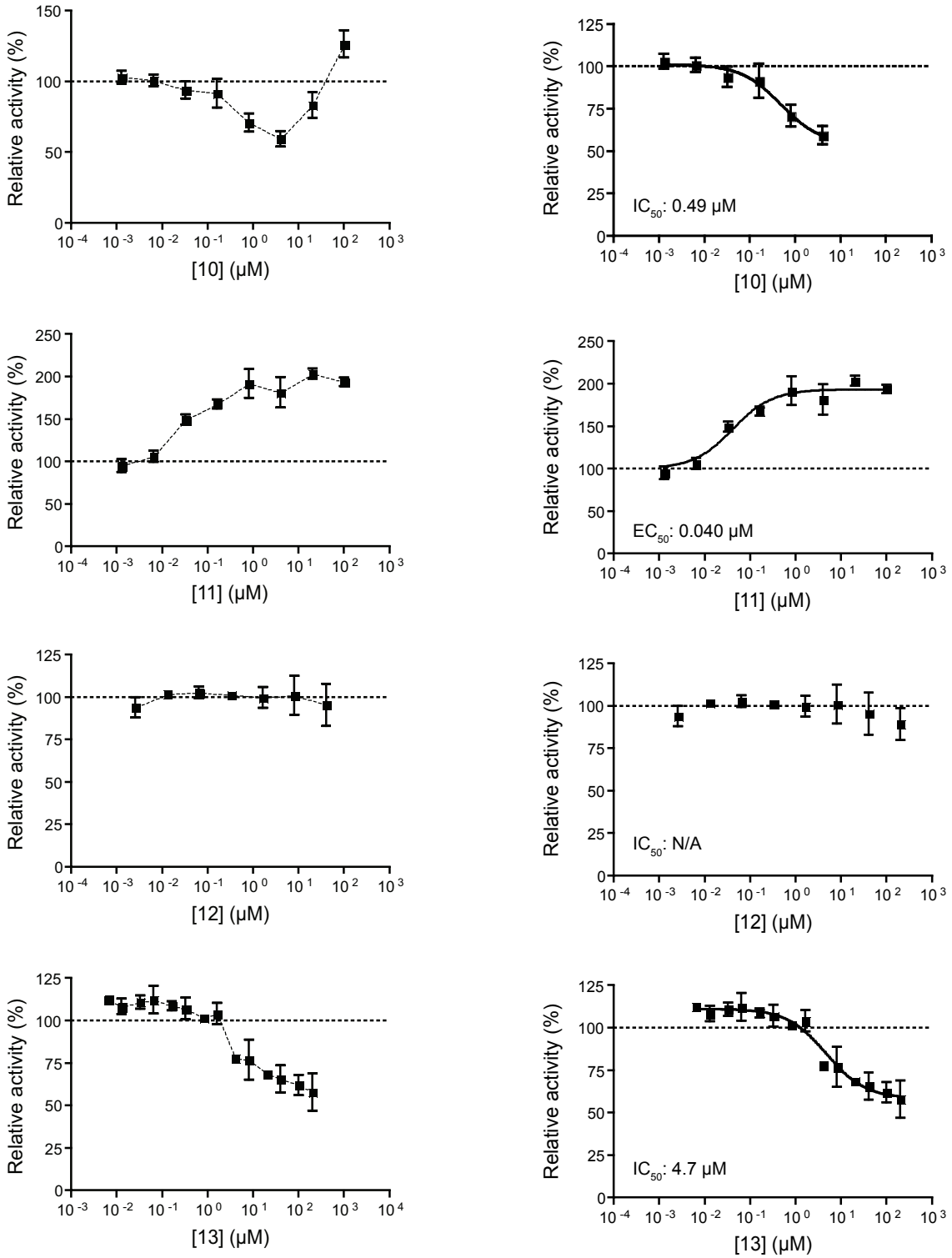

Figure S3 (continued): LasR antagonism dose responses and IC_{50} values (or EC_{50} values, for compounds that activated more strongly than OdDHL) for all tested compounds in the *E. coli* JLD271 *lasI-lacZ* reporter strain. Plots on left show the full dose–response including non-monotonic behavior, if applicable. Plots on right are truncated (if necessary) to show the dose–response curves of the concentration regime where LasR inhibition was observed. Compounds were screened against 2 nM OdDHL. IC_{50} values and the EC_{50} value were calculated from the plots on right using GraphPad Prism. Error bars, SEM of n = 3 trials.

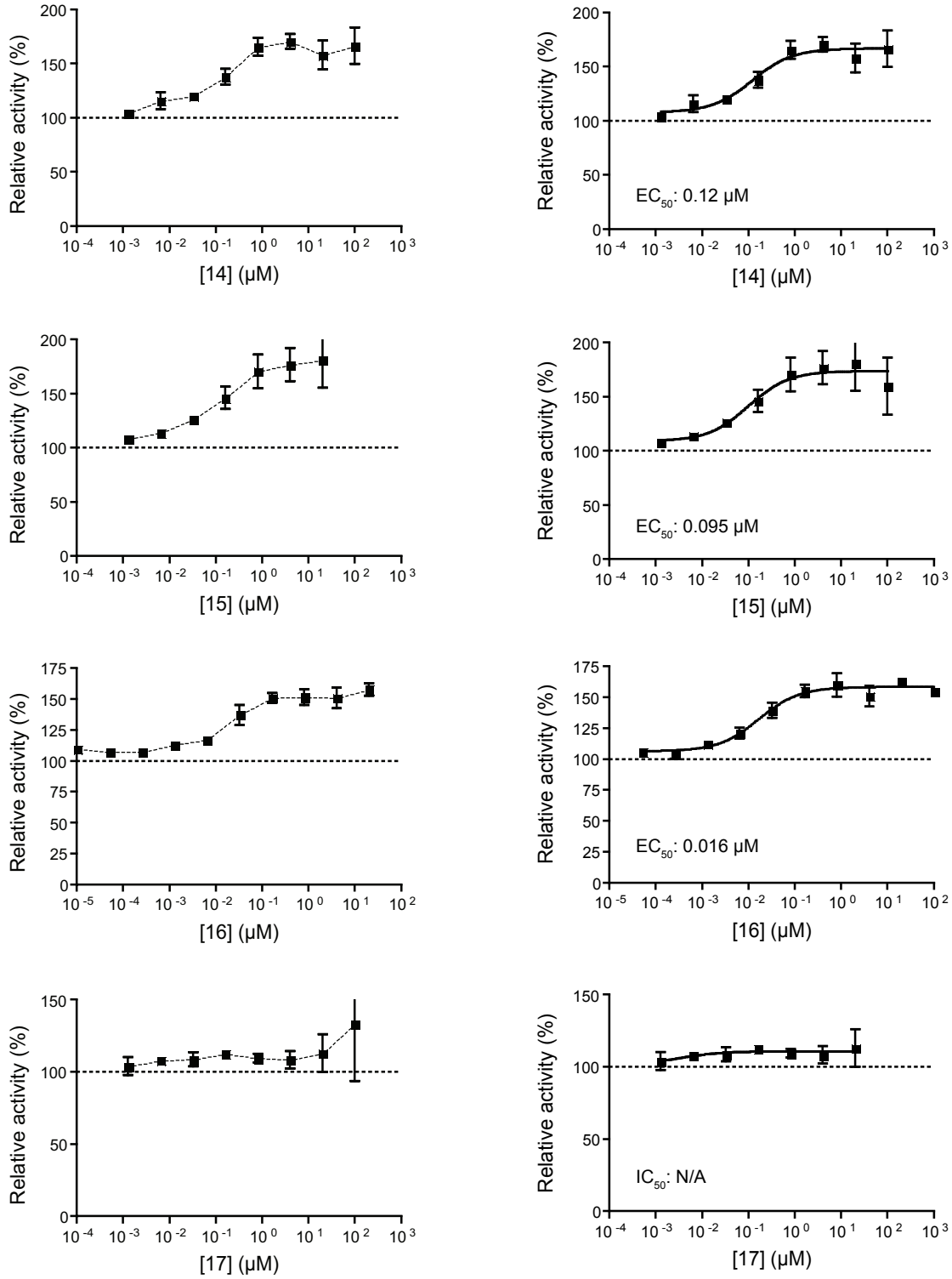

Figure S3 (continued): LasR antagonism dose responses and EC_{50} values (for compounds that activated more strongly than OdDHL) for all tested compounds in the *E. coli* JLD271 *lasI-lacZ* reporter strain. Plots on left show the full dose–response. Plots on right are fitted to a sigmoidal curve. Compounds were screened against 2 nM OdDHL. Where possible, EC_{50} values were calculated from the plots on right using GraphPad Prism. Error bars, SEM of n = 3 trials.

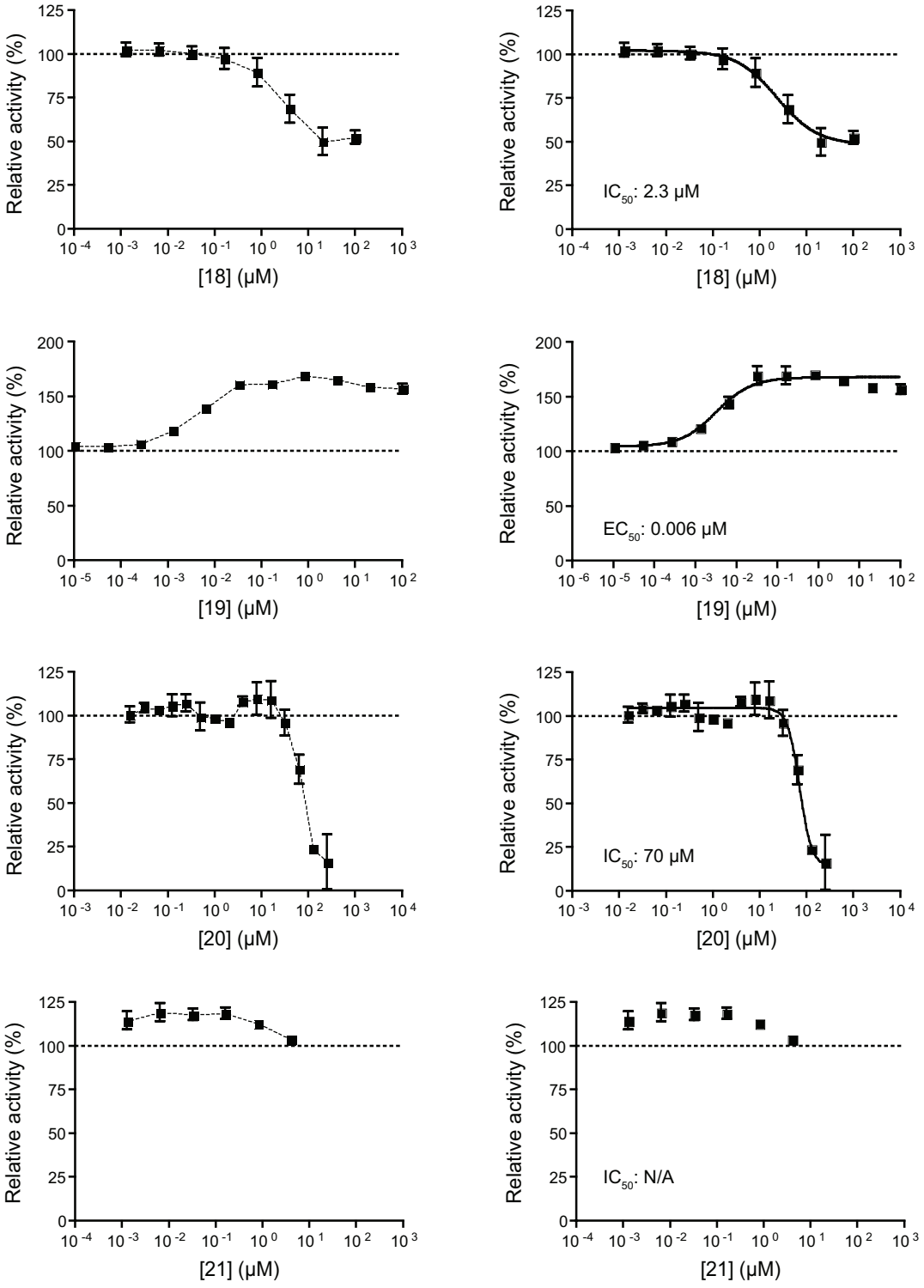

Figure S3 (continued): LasR antagonism dose responses and IC_{50} values (or EC_{50} values, for compounds that activated more strongly than OdDHL) for all tested compounds in the *E. coli* JLD271 *lasI-lacZ* reporter strain. Plots on left show the full dose–response. Plots on right are fitted to a sigmoidal curve. Compounds were screened against 2 nM OdDHL. Where possible, IC_{50} values and the EC_{50} value were calculated from the plots on right using GraphPad Prism. Error bars, SEM of n = 3 trials.

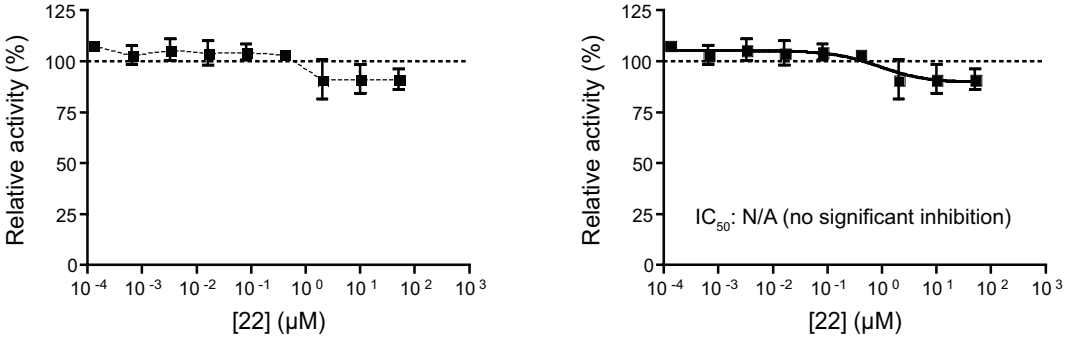

Figure S3 (continued): LasR antagonism dose responses and IC_{50} values for all tested compounds in the *E. coli* JLD271 *lasI-lacZ* reporter strain. The plot on left shows the full dose–response. The plot on right is fitted to a sigmoidal curve. Compounds were screened against 2 nM OdDHL. Error bars, SEM of n = 3 trials.

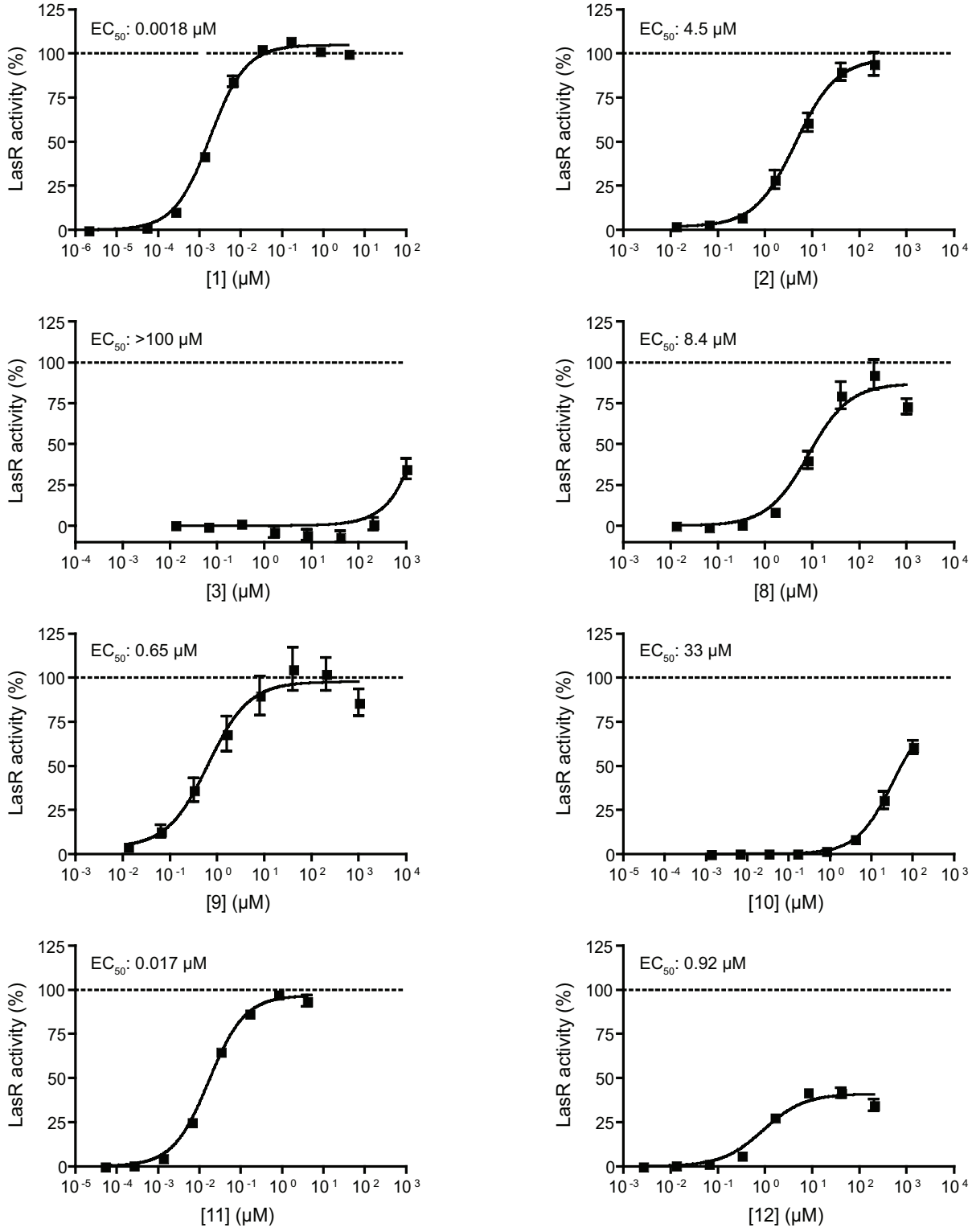

Figure S4*:* LasR agonism dose responses and EC_{50} values for all tested compounds in the *E. coli* JLD271 *lasI-lacZ* reporter strain. EC_{50} values were calculated using GraphPad Prism. Error bars, SEM of n = 3 trials.

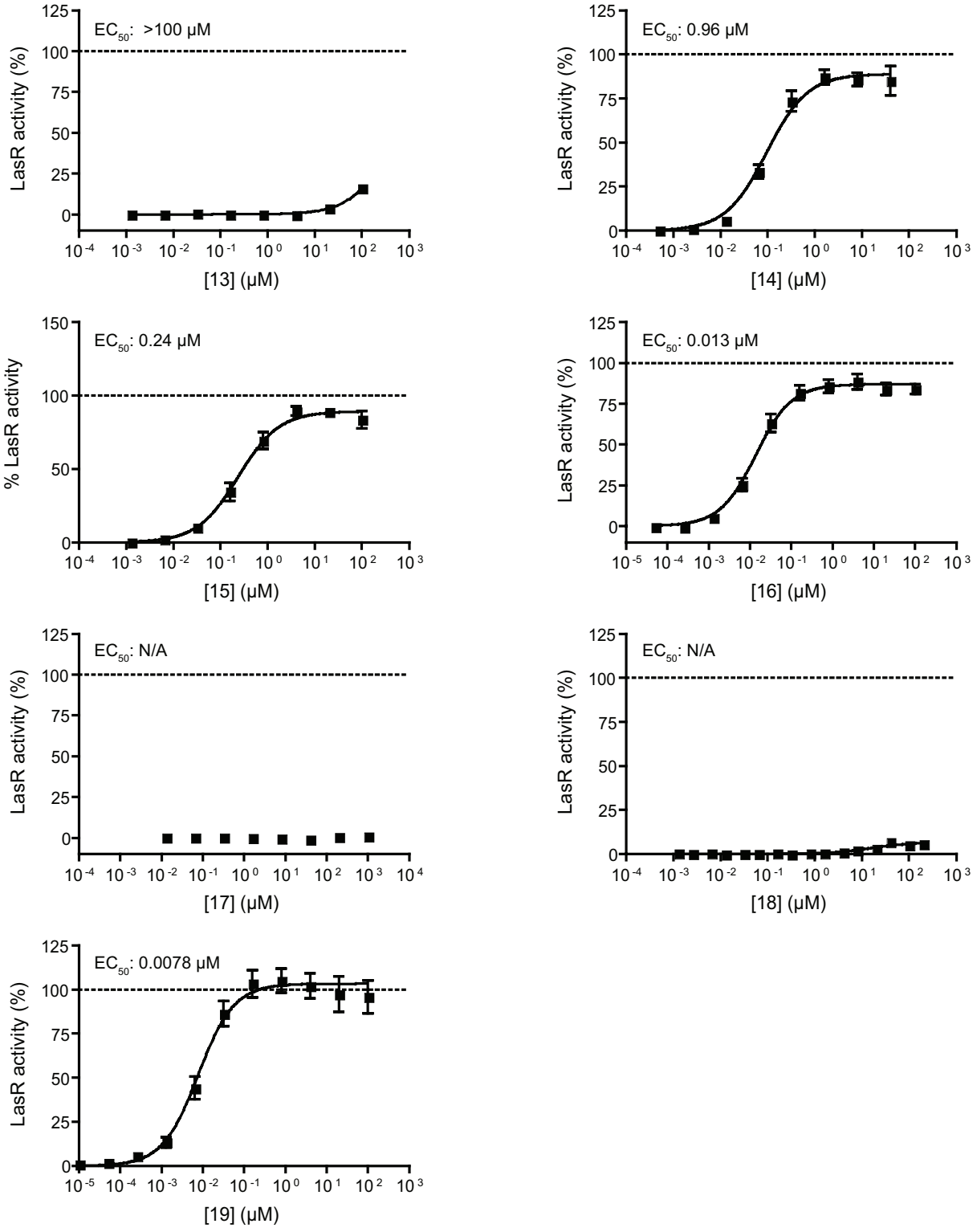

Figure S4 (continued): LasR agonism dose responses and EC_{50} values for all tested compounds in the *E. coli* JLD271 *lasI-lacZ* reporter strain. Where possible, EC_{50} values were calculated using GraphPad Prism. Error bars, SEM of n = 3 trials.

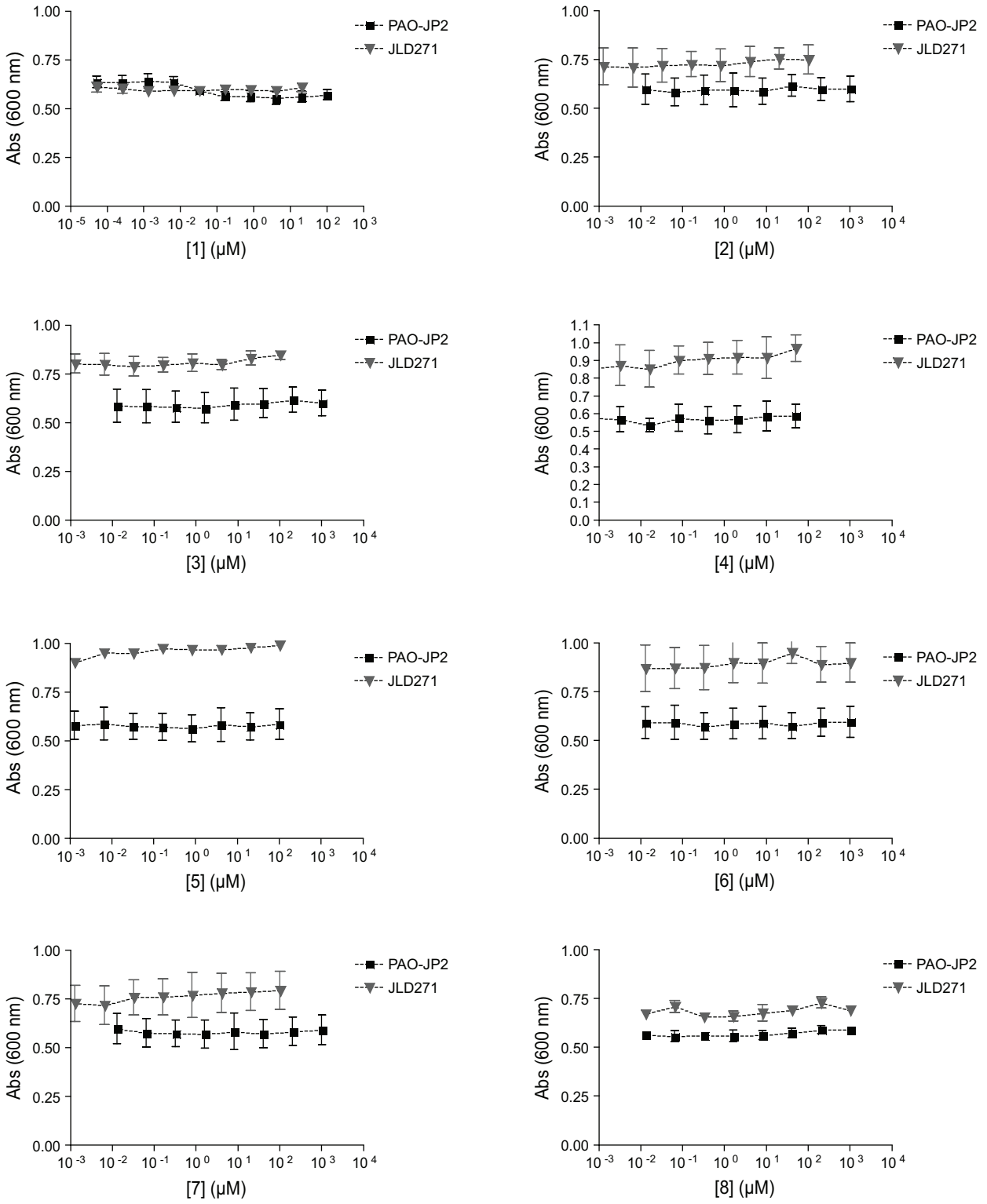

Figure S5*:* Endpoint growth (OD_{600}) data for library compounds at all tested concentrations in the *P. aeruginosa* PAO-JP2 and *E. coli* JLD271 reporter strains.

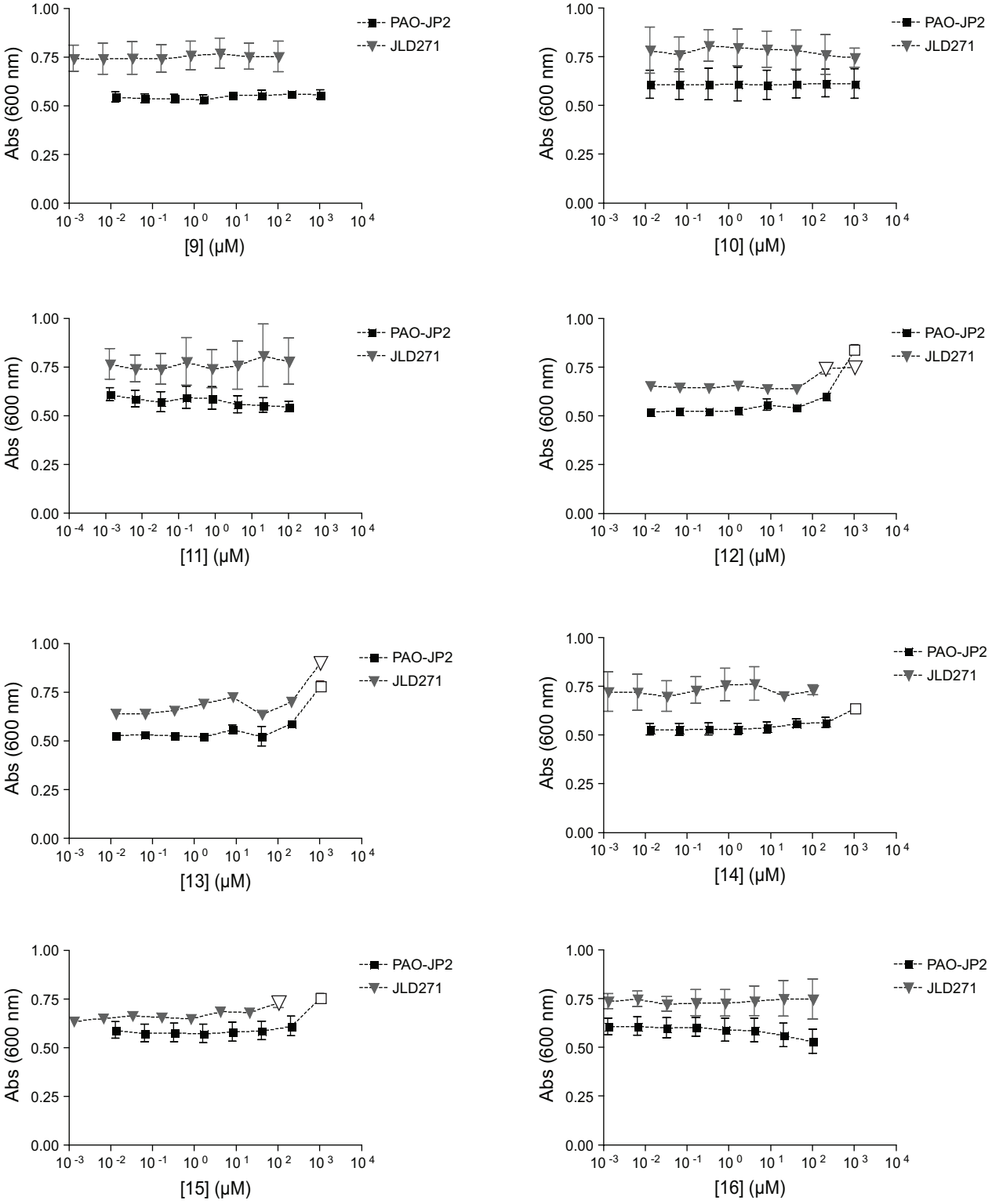

Figure S5 (continued): Endpoint growth (OD_{600}) data for library compounds at all tested concentrations in the *P. aeruginosa* PAO-JP2 and *E. coli* JLD271 reporter strains. Unfilled data points were statistically significant outliers and were thus excluded from LasR dose–response analysis.

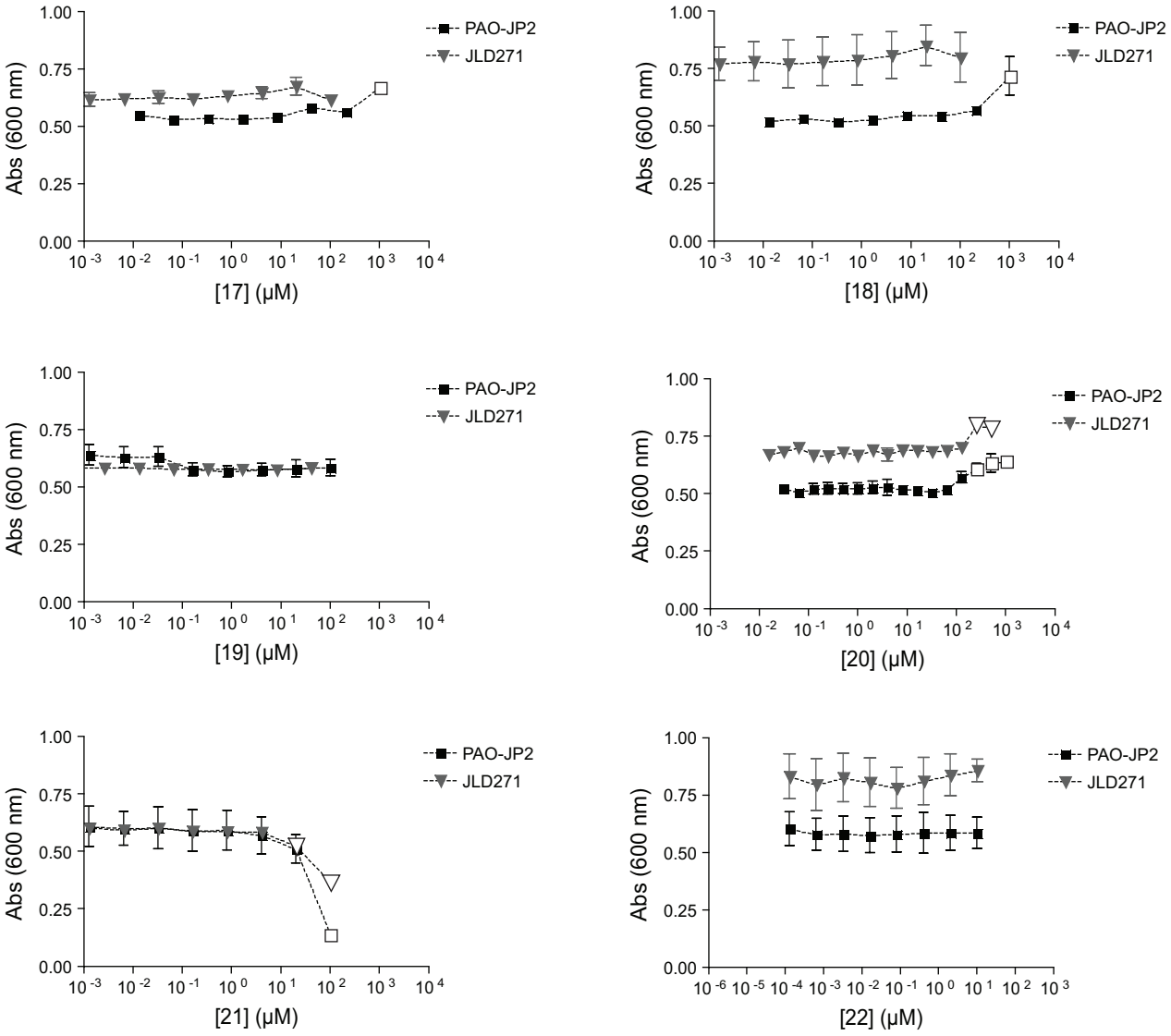

Figure S5 (continued)*:* Endpoint growth (OD_{600}) data for library compounds at all tested concentrations in the *P. aeruginosa* PAO-JP2 and *E. coli* JLD271 LasR reporter strains. Unfilled data points were statistically significant outliers and were thus excluded from LasR dose–response analysis.

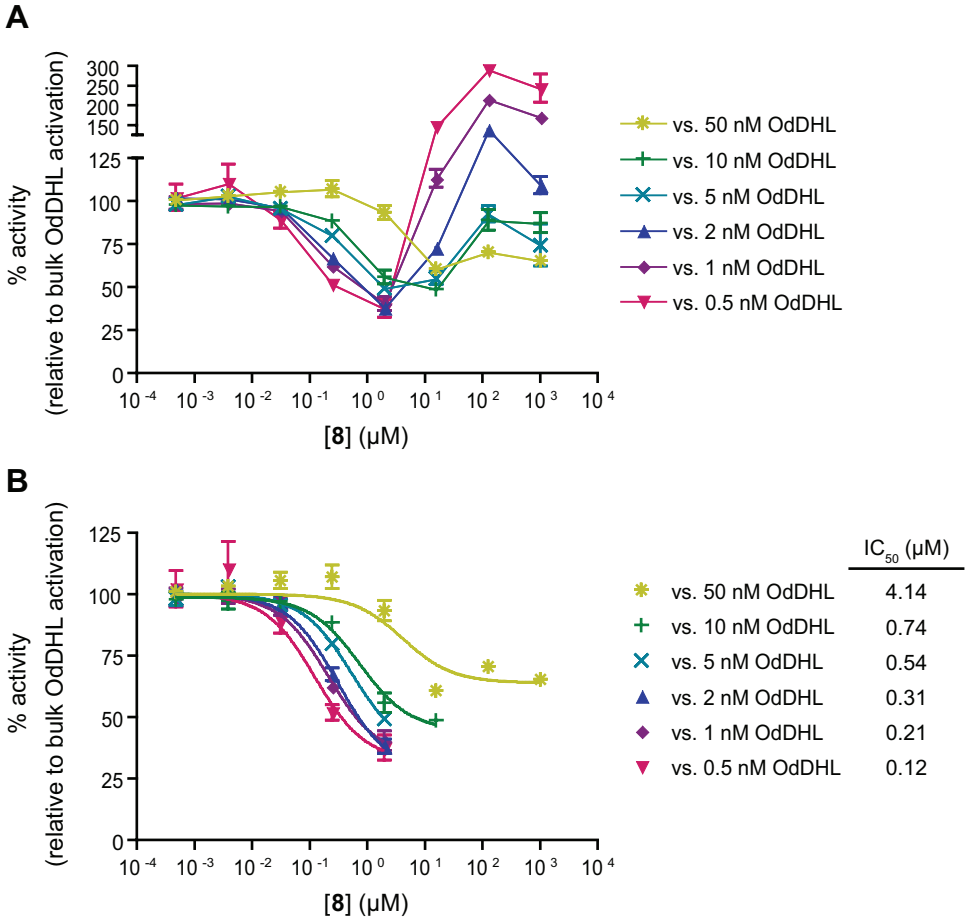

Figure S6*:* Two-dimensional dose–response study of compound **8** vs. LasR native ligand **1** (OdDHL) in the *E. coli* LasR reporter JLD271 + pJN105L + pSC11. Plot (A) shows curves adjusted relative to activity elicited by bulk **1** (OdDHL) in each trial. Plot (B) shows curves that were adjusted and truncated to more clearly show the shift of IC_{50} against increasing amounts of **1** (OdDHL). Error bars: SEM of n = 3 trials.

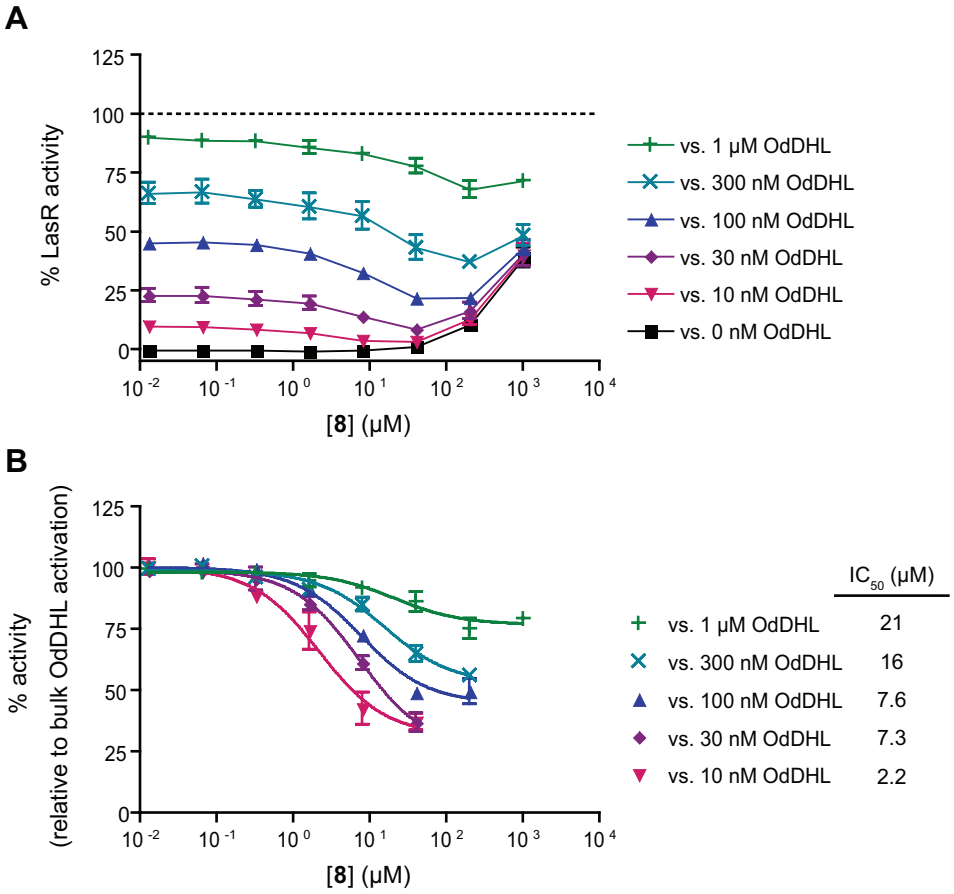

Figure S7*:* Two-dimensional dose–response study in the *P. aeruginosa* LasR reporter PAO-JP2 + p*lasI*-LVA*gfp* of compound **8** vs. LasR native ligand **1** (OdDHL). Non-classical partial agonist behavior is conserved in the *P. aeruginosa* LasR reporter PAO-JP2 + p*lasI*-LVA*gfp*. In plot (A), a two-dimensional dose–response study of compound **8** vs. **1** (OdDHL) shows competitive antagonism and non-competitive agonism. The antagonistic behavior of **8** (at concentrations < 100 μM) is competitive with **1** (OdDHL) and shifts to higher IC_{50} when competed against higher concentrations of **1** (OdDHL). The partial agonist behavior of **8** (at concentrations > 100 μM), on the other hand, is insurmountable with increasing concentrations of **1** (OdDHL). In plot (B), curves were adjusted relative to activity elicited by bulk (**1**) OdDHL in each trial and truncated to more clearly show the shift of antagonistic potency against increasing amounts of **1** (OdDHL). IC_{50} values for **8** at variable concentrations of **1** (OdDHL) are listed. Error bars: SEM of n = 3 trials.

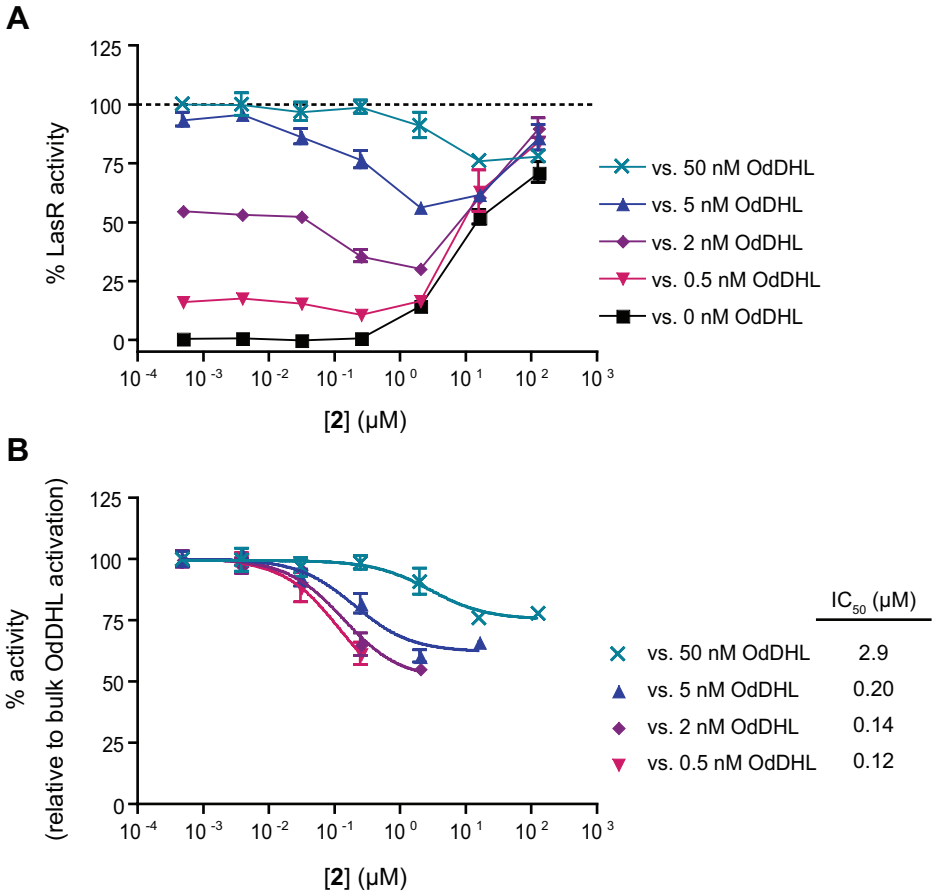

Figure S8*:* Two-dimensional dose–response study in *E. coli* LasR reporter JLD271 + pJN105L + pSC11 of compound **2** vs. LasR native ligand **1** (OdDHL). Compound **2**, despite structural differences, shows analogous bimodal behavior as compound **8**. In plot (A), the antagonistic behavior of **2** (at concentrations < 10 μM) is competitive with **1** (OdDHL) and shifts to higher IC_{50} when competed against higher concentrations of **1** (OdDHL). The partial agonist behavior of **2** (at concentrations > 10 μM), on the other hand, is insurmountable with increasing concentrations of **1** (OdDHL). In plot (B), curves were adjusted relative to activity elicited by bulk **1** (OdDHL) in each trial and truncated to more clearly show the shift of antagonistic potency against increasing amounts of **1** (OdDHL). IC_{50} values for **2** at variable concentrations of **1** (OdDHL) are listed. Error bars: SEM of n = 3 trials

Table S4*:* Full comparison, including statistical analysis, of LasR antagonist and agonist potency shifts between pump-active (PAO-JP2) and pump-mutant (PAO-JG21) *P. aeruginosa* LasR reporter strains.[a]

	Antagonism			
Compound	PAO-JP2 IC_{50} (μM)	PAO-JG21 IC_{50} (μM)	Fold Change[b]	P value
2 (OOHL)	5.5	0.57	9.6	<0.0001
3 (OHHL)	40	41	**1.0**	**0.88**
4	≥100	≥20	–	–
5	73	8.9	8.2	<0.0001
6	175	20	8.8	<0.0001
7	116	8.2	14.1	<0.0001
8	12	1.5	8.0	0.0012
9	3	0.42	7.1	0.0006
10 (CL)	21	1.3	16.2	<0.0001
11 (ITC-12)	No inhibition	No inhibition	–	–
12	9.7	3.7	2.6	<0.0002
13	>200	≥50	–	–
14	No activity	No activity	–	–
15	≥100	No activity	–	–
16 (mBTL)	No inhibition	No inhibition	–	–
17 (C10-CPA)	≥50	>100	–	–
18 (V-06-018)	5.2	6.1	**0.9**	**0.46**
19 (TP-1)	No inhibition	No inhibition	–	–
20 (TP-5)	69	63	**1.1**	**0.79**
21 (C-30)	No activity	No activity	–	–
22 (PD-12)	2.5	0.11	22.7	0.016

	Agonism			
Compound	PAO-JP2 EC_{50} (μM)	PAO-JG21 EC_{50} (μM)	Fold Change[b]	P value
1 (OdDHL)	0.1393	0.0189	7.4	<0.0001
2	>200	26	>7.7	<0.0001
8	>200	24	>8.3	<0.0001
9	140	8.6	16.3	<0.0001
11 (ITC-12)	2.6	1.3	2.0	0.0005
14	17	15	**1.1**	**0.92**
15	>200	>200	–	–
16 (mBTL)	4.2	0.56	7.5	<0.0001
19 (TP-1)	0.071	0.036	2.0	0.027

[a] Both *P. aeruginosa* strains utilize the plasmid *plasI*-LVA*gfp* to report LasR activity.
[b] Compounds with statistically insignificant shifts in potency ($p > 0.1$) are shown in bold.

Table S5*:* Comparison of LasR antagonist and agonist potencies between the *P. aeruginosa* pump-active (PAO-JP2), *P. aeruginosa* pump-mutant (PAO-JG21), and *E. coli* (JLD271) LasR reporter strains.[a]

	Antagonism potency			**Potency shift (fold-change)**	
Compound	PAO-JP2 IC_{50} (μM)	PAO-JG21 IC_{50} (μM)	JLD271 IC_{50} (μM)	PAO-JP2/ PAO-JG21	PAO-JP2/ JLD271
2 (OOHL)	5.5	0.57	0.078	9.6	71
3 (OHHL)	40	41	10.4	1.0	3.8
4	≥100	≥20	2.8	–	–
5	73	8.9	2.8	8.2	26
6	175	20	1.0	8.8	180
7	116	8.2	3.5	14	33
8	12	1.5	0.16	8.0	75
9	3	0.42	No inhibition	7.1	–
10 (CL)	21	1.3	0.49	16	43
11 (ITC-12)	No inhibition	No inhibition	No inhibition	–	–
12	9.7	3.7	No activity	2.6	–
13	>200	≥50	4.7	–	–
14	No activity	No activity	No inhibition	–	–
15	≥100	No activity	No inhibition	–	–
16 (mBTL)	No inhibition	No inhibition	No inhibition	–	–
17 (C10-CPA)	≥50	>100	No activity	–	–
18 (V-06-018)	5.2	6.1	2.3	0.9	2.3
19 (TP-1)	No inhibition	No inhibition	No inhibition	–	–
20 (TP-5)	69	63	70	1.1	1.0
21 (C-30)	No activity	No activity	No activity	–	–
22 (PD-12)	2.5	0.11	No activity	23	–

	Agonism potency			**Potency shift (fold-change)**	
Compound	PAO-JP2 EC_{50} (μM)	PAO-JG21 EC_{50} (μM)	JLD271 EC_{50} (μM)	PAO-JP2/ PAO-JG21	PAO-JP2/ JLD271
1 (OdDHL)	0.1393	0.0189	0.0018	7.4	77
2	>200	26	4.5	–	–
8	>200	24	8.4	–	–
9	140	8.6	0.65	16	220
11 (ITC-12)	2.6	1.3	0.017	2.0	150
14	17	15	0.096	1.1	180
15	>200	>200	0.24	–	–
16 (mBTL)	4.2	0.56	0.013	7.5	320
19 (TP-1)	0.071	0.036	0.0078	2.0	9.1

[a] Both *P. aeruginosa* reporter strains utilize the plasmid *plasI*-LVA*gfp* to report LasR activity. The *E. coli* JLD271 reporter strain utilizes the plasmid pSC-11 to report LasR activity.

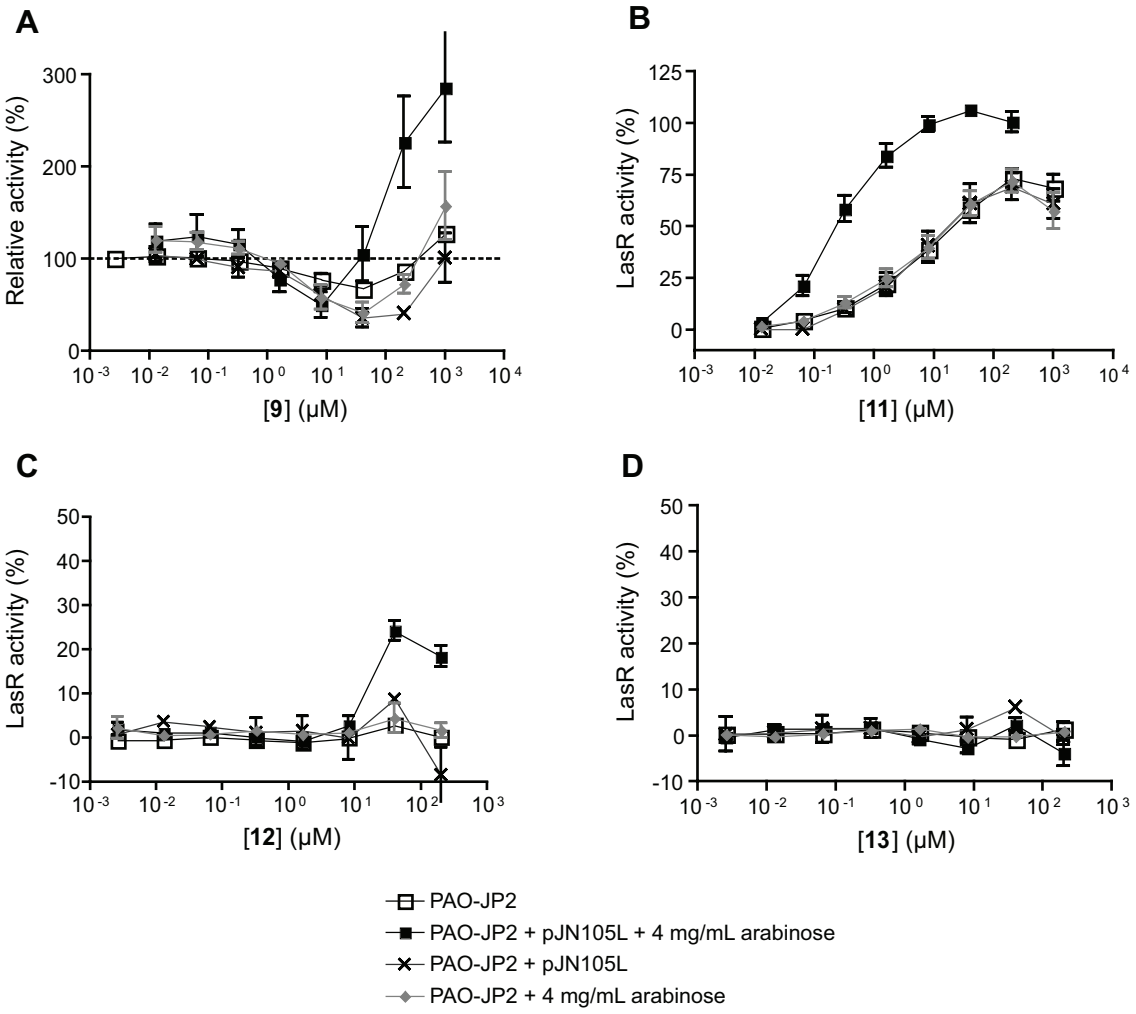

Figure S9*:* Control experiments for dose–response assays using the *P. aeruginosa* PAO-JP2 LasR reporter harboring the LasR expression plasmid pJN105L. Dose-response antagonism assays for compound **9** (A), and dose–response agonism assays for **11** (B), **12** (C), and **13** (D) were performed as described in the Experimental Section. Controls included adding 4 mg/mL L-arabinose to the PAO-JP2 LasR reporter strain without the LasR expression plasmid (dark-grey X), and omitting addition of L-arabinose to the PAO-JP2 LasR reporter harboring the LasR expression plasmid pJN105L (grey diamond). Error bars: SEM of n = 3 trials.

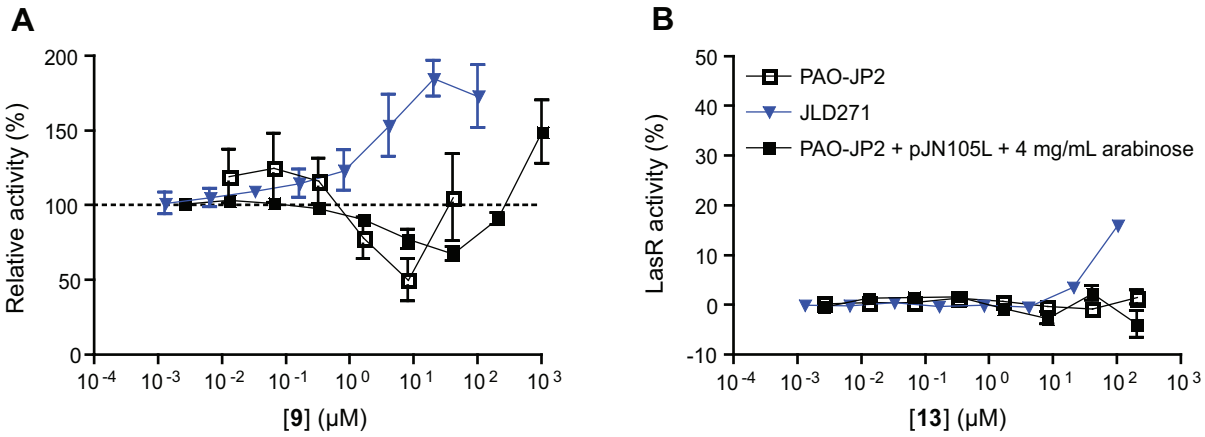

Figure S10*:* Dose–response behaviors of compounds **9** (A) and **13** (B) in a *P. aeruginosa* LasR overexpression/reporter strain (filled squares) compared to a native expression LasR reporter strain (empty squares) and a heterologous *E. coli* LasR reporter strain (blue triangles). The plasmid pJN105L used for LasR expression in the *E. coli* reporter was transformed into the *P. aeruginosa* PAO-JP2 LasR reporter and induced using 4 mg/mL arabinose. Error bars: SEM of n = 3 trials.

Note S7*:* Proposed hypotheses for the behaviors of compounds **9** and **13** in LasR overexpression reporters.

For non-classical partial agonist **9**, the response of the *P. aeruginosa* reporter overexpressing LasR did not match that of either the *E. coli* LasR reporter or the *P. aeruginosa* native LasR expression reporter. We see that the overall non-classical bimodal activity was conserved in the *P. aeruginosa* LasR overexpression reporter, but the potency of the *agonistic* binding event was altered by LasR overexpression (*i.e.*, the upturn to agonistic activity occurs at lower concentrations). We propose in Mechanistic Insight 1 (see main text) that the agonistic and antagonistic binding events for these non-classical partial agonists are occurring at discrete locations (i.e., one event at the LasR ligand-binding site and the second event at either an allosteric LasR site or a separate target (or targets)); thus, it may be the case that overexpression of LasR more strongly perturbs the potency pertaining to the agonistic binding event. For example, if this agonistic event for **9** occurs at the dimerization interface of two LasR monomers, the agonistic binding event may be more strongly dependent on LasR concentration than the competitive antagonistic binding event. If this effect is magnified in the *E. coli* LasR reporter (which also overexpresses LasR), the agonistic event could be potent enough to completely subsume the antagonistic event.

Compound **13** showed no activity in the *P. aeruginosa* reporter overexpressing LasR at any concentration tested, despite it displaying modest agonistic activity in the *E. coli* LasR reporter. We hypothesize that this apparent lack of activity is largely due to the decreased potency of **13** in *P. aeruginosa* strains overall, as a result of increased active efflux and decreased membrane permeability relative to *E. coli*.

Table S6: Comparison of *P. aeruginosa* PAO1 elastase B production in the presence of LasR modulators.[a]

Compound	Relative elastase production (%)	QS-dependent elastase production (%)	Statistical significance from DMSO control[b]	Statistical significance from Δ*lasIrhlI* control[b]
DMSO	100.0	100.0	–	$P < 0.01$
7	82.3	73.0	$P > 0.05$	$P < 0.01$
8	94.9	92.2	$P > 0.05$	$P < 0.01$
11	225.3	291.3	$P < 0.01$	$P < 0.01$
12	68.0	51.1	$P < 0.05$	$P < 0.05$
13	42.4	12.0	$P < 0.01$	**$P > 0.05$**
16	189.9	237.3	$P < 0.01$	$P < 0.01$
18	44.3	15.0	$P < 0.01$	**$P > 0.05$**
19	126.4	140.4	$P > 0.05$	$P < 0.01$
20	69.8	54.0	$P < 0.05$	$P < 0.01$
22	70.9	55.6	$P < 0.05$	$P < 0.01$
Δ*lasIrhlI*	34.5	0.0	$P < 0.01$	–

[a] See Experimental Section and Table S1 for full assay and strain information. Compounds were screened at 100 μM. Relative elastase production was measured by normalizing elastase production to that in wells containing only DMSO. QS-dependent elastase production was background corrected to that of the Δ*lasIrhlI* strain and normalized as above.

[b] P values were calculated using one-way ANOVA and Dunnett's multiple comparison post-test. Bold values represent statistical insignificance between compound-treated and QS-null elastase production.

References.

(1) Holloway, B. W. *J. Gen. Microbiol.* **1955**, *13*, 572-581.

(2) Pearson, J.; Pesci, E.; Iglewski, B. *J. Bacteriol.* **1997**, *179*, 5756-5767.

(3) Moore, J. D.; Gerdt, J. P.; Eibergen, N. R.; Blackwell, H. E. *ChemBioChem* **2014**, *15*, 435-442.

(4) Lindsay, A.; Ahmer, B. M. M. *J. Bacteriol.* **2005**, *187*, 5054-5058.

(5) Simon, R.; O'Connell, M.; Labes, M.; Puhler, A. *Methods Enzymol.* **1986**, *118*, 640-659.

(6) de Kievit, T. R.; Gillis, R.; Marx, S.; Brown, C.; Iglewski, B. H. *Appl. Environ. Microbiol.* **2001**, *67*, 1865-1873.

(7) Chugani, S. A.; Whiteley, M.; Lee, K. M.; D'Argenio, D.; Manoil, C.; Greenberg, E. P. *Proc. Natl. Acad. Sci. U. S. A.* **2001**, *98*, 2752-2757.

(8) Lee, J. H.; Lequette, Y.; Greenberg, E. P. *Mol. Microbiol.* **2006**, *59*, 602-609.

(9) Mattmann, M. E.; Blackwell, H. E. *J. Org. Chem.* **2010**, *75*, 6737-6746.

(10) Galloway, W.; Hodgkinson, J. T.; Bowden, S. D.; Welch, M.; Spring, D. R. *Chem. Rev.* **2011**, *111*, 28-67.

(11) Miller, M. B.; Bassler, B. L. *Annu. Rev. Microbiol.* **2001**, *55*, 165-199.

(12) Zhu, J.; Beaber, J. W.; More, M. I.; Fuqua, C.; Eberhard, A.; Winans, S. C. *J. Bacteriol.* **1998**, *180*, 5398-5405.

(13) Reverchon, S.; Chantegrel, B.; Deshayes, C.; Doutheau, A.; Cotte-Pattat, N. *Bioorg. Med. Chem. Lett.* **2002**, *12*, 1153-1157.

(14) Geske, G. D.; O'Neill, J. C.; Miller, D. M.; Mattmann, M. E.; Blackwell, H. E. *J. Am. Chem. Soc.* **2007**, *129*, 13613-13625.

(15) Geske, G. D.; Wezeman, R. J.; Siegel, A. P.; Blackwell, H. E. *J. Am. Chem. Soc.* **2005**, *127*, 12762-12763.

(16) Geske, G. D.; Mattmann, M. E.; Blackwell, H. E. *Bioorg. Med. Chem. Lett.* **2008**, *18*, 5978-5981.

(17) Chen, G.; Swem, L. R.; Swem, D. L.; Stauff, D. L.; O'Loughlin, C. T.; Jeffrey, P. D.; Bassler, B. L.; Hughson, F. M. *Mol. Cell* **2011**, *42*, 199-209.

(18) Swem, L. R.; Swem, D. L.; O'Loughlin, C. T.; Gatmaitan, R.; Zhao, B.; Ulrich, S. M.; Bassler, B. L. *Mol. Cell* **2009**, *35*, 143-153.

(19) O'Loughlin, C. T.; Miller, L. C.; Siryaporn, A.; Drescher, K.; Semmelhack, M. F.; Bassler, B. L. *Proc. Natl. Acad. Sci. U. S. A.* **2013**, *110*, 17981-17986.

(20) Amara, N.; Mashiach, R.; Amar, D.; Krief, P.; Spieser, S. A. H.; Bottomley, M. J.; Aharoni, A.; Meijler, M. M. *J. Am. Chem. Soc.* **2009**, *131*, 10610-10619.

(21) McInnis, C. E.; Blackwell, H. E. *Bioorg. Med. Chem.* **2011**, *19*, 4812-4819.

(22) Hodgkinson, J. T.; Galloway, W. R.; Wright, M.; Mati, I. K.; Nicholson, R. L.; Welch, M.; Spring, D. R. *Org. Biomol. Chem.* **2012**, *10*, 6032-6044.

(23) Smith, K. M.; Bu, Y.; Suga, H. *Chem. Biol.* **2003**, *10*, 563-571.

(24) Smith, K. M.; Bu, Y.; Suga, H. *Chem. Biol.* **2003**, *10*, 81-89.

(25) Welsh, M. A.; Eibergen, N. R.; Moore, J. D.; Blackwell, H. E. *J. Am. Chem. Soc.* **2015**, *137*, 1510-1519.

(26) Ishida, T.; Ikeda, T.; Takiguchi, N.; Kuroda, A.; Ohtake, H.; Kato, J. *Appl. Environ. Microbiol.* **2007**, *73*, 3183-3188.

(27) Müh, U.; Schuster, M.; Heim, R.; Singh, A.; Olson, E. R.; Greenberg, E. P. *Antimicrob. Agents Chemother.* **2006**, *50*, 3674-3679.

(28) Muh, U.; Hare, B. J.; Duerkop, B. A.; Schuster, M.; Hanzelka, B. L.; Heim, R.; Olson, E. R.; Greenberg, E. P. *Proc. Natl. Acad. Sci. U. S. A.* **2006**, *103*, 16948-16952.

(29) Zou, Y.; Nair, S. K. *Chem. Biol.* **2009**, *16*, 961-970.

(30) Bottomley, M. J.; Muraglia, E.; Bazzo, R.; Carfi, A. *J. Biol. Chem.* **2007**, *282*, 13592-13600.

(31) Hentzer, M.; Wu, H.; Andersen, J. B.; Riedel, K.; Rasmussen, T. B.; Bagge, N.; Kumar, N.; Schembri, M. A.; Song, Z.; Kristoffersen, P.; Manefield, M.; Costerton, J. W.; Molin, S.; Eberl, L.; Steinberg, P.; Kjelleberg, S.; Hoiby, N.; Givskov, M. *EMBO J.* **2003**, *22*, 3803-3815.

(32) Wu, H.; Song, Z.; Hentzer, M.; Andersen, J. B.; Molin, S.; Givskov, M.; Høiby, N. *J. Antimicrob. Chemother.* **2004**, *53*, 1054-1061.

(33) El-Mowafy, S. A.; Abd El Galil, K. H.; El-Messery, S. M.; Shaaban, M. I. *Microb. Pathog.* **2014**, *74*, 25-32.

(34) Yang, L.; Rybtke, M. T.; Jakobsen, T. H.; Hentzer, M.; Bjarnsholt, T.; Givskov, M.; Tolker-Nielsen, T. *Antimicrob. Agents Chemother.* **2009**, *53*, 2432-2443.

(35) Costas, C.; Lopez-Puente, V.; Bodelon, G.; Gonzalez-Bello, C.; Perez-Juste, J.; Pastoriza-Santos, I.; Liz-Marzan, L. M. *ACS Nano* **2015**, *9*, 5567-5576.

(36) Morkunas, B.; Galloway, W. R.; Wright, M.; Ibbeson, B. M.; Hodgkinson, J. T.; O'Connell, K. M.; Bartolucci, N.; Della Valle, M.; Welch, M.; Spring, D. R. *Org. Biomol. Chem.* **2012**, *10*, 8452-8464.

(37) Zakhari, J. S.; Kinoyama, I.; Struss, A. K.; Pullanikat, P.; Lowery, C. A.; Lardy, M.; Janda, K. D. *J. Am. Chem. Soc.* **2011**, *133*, 3840-3842.

(38) Persson, T.; Hansen, T. H.; Rasmussen, T. B.; Skinderso, M. E.; Givskov, M.; Nielsen, J. *Org. Biomol. Chem.* **2005**, *3*, 253-262.

(39) Griffith, K. L.; Wolf Jr., R. E. *Biochem. Biophys. Res. Commun.* **2002**, *290*, 397-402.

(40) Defoirdt, T.; Brackman, G.; Coenye, T. *Trends Microbiol.* **2013**, *21*, 619-624.

(41) Baell, J. B.; Walters, M. A. *Nature* **2014**, *513*, 481-483.

HPLC and MS Data.

HPLC and MS data were obtained for all compounds in this study that were purchased from commercial sources (**1**–**4**, **15**, and **21**), donated by other research laboratories (**11** and **19**), or reported by other laboratories but synthesized in our laboratory (**10**, **13**, **16**–**18**, **20**, and **22**).

HPLC instrumentation and methods. Reversed-phase high-performance liquid chromatography (RP-HPLC) was performed using a Shimadzu system equipped with an SCL-10Avp controller, an LC-10AT pump, an FCV-10ALvp solvent mixer, and an SPD-M10Avp UV-vis diode array detector. A Zorbax Rx-C8 column (5 μm, 4.6 mm x 250 mm) was used for analytical RP-HPLC. HPLC conditions were as follows: flow rates = 1 mL min^{-1}; mobile phase A = 18 MΩ water + 0.1% trifluoroacetic acid (TFA); mobile phase B = acetonitrile + 0.1% TFA; linear gradient 15% to 95% B over 27 min. Purities were determined by integration of peaks with UV detection at 214 nm. These integration values are indicated above the peaks in the traces below (ranging from 94.4–100%).

MS instrumentation and methods. Exact mass measurements were obtained using a Waters LCT electrospray ionization (ESI) TOF mass spectrometer. Samples were dissolved in acetonitrile and sprayed with a cone voltage of 20 V. The purchase of the LCT spectrometer by the UW–Madison Department of Chemistry was partially funded by NSF Award CHE-9974839.

1: ESI-MS calculated m/z $[M+1]^+$ 298.2013, observed m/z $[M+1]^+$ 298.2007

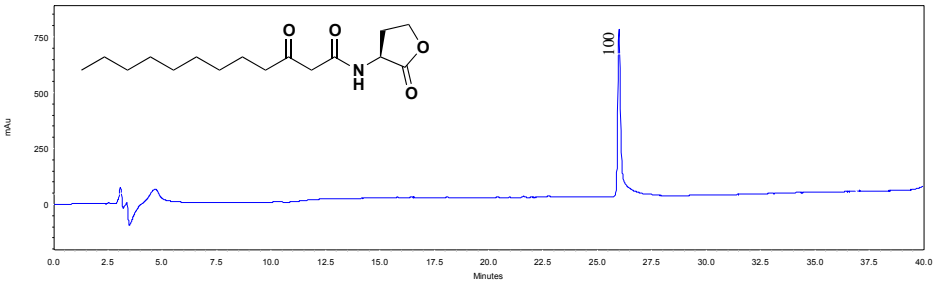

2: ESI-MS calculated m/z $[M+1]^+$ 242.1387, observed m/z $[M+1]^+$ 242.1382

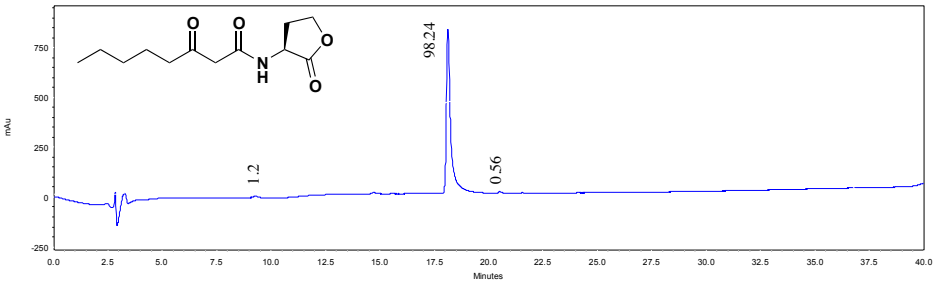

3: ESI-MS calculated m/z $[M+1]^+$ 214.1074, observed m/z $[M+1]^+$ 214.1071

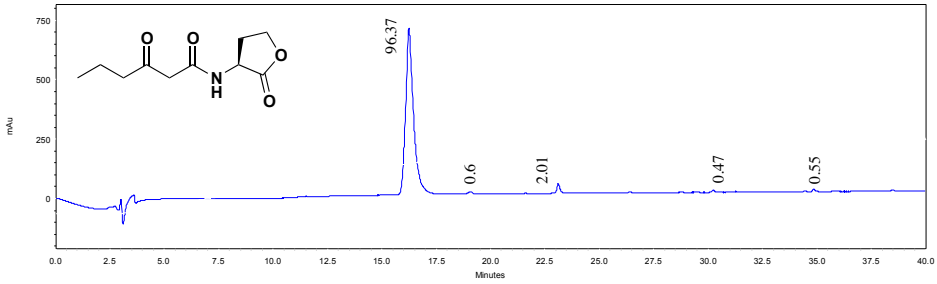

4: ESI-MS calculated m/z $[M+1]^+$ 214.1438, observed m/z $[M+1]^+$ 214.1435

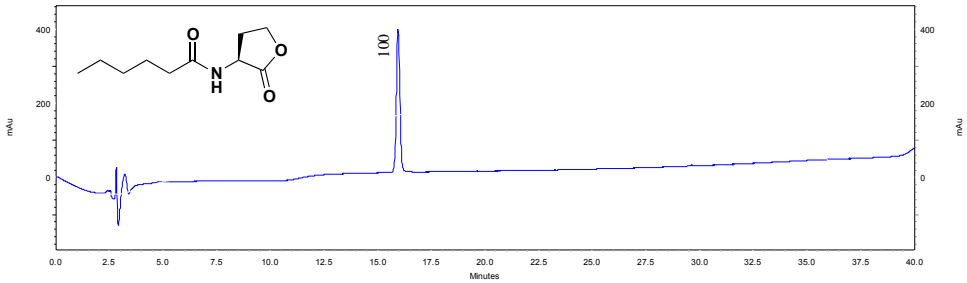

10: ESI-MS calculated m/z $[M+1]^+$ 298.0841, observed m/z $[M+1]^+$ 298.0836

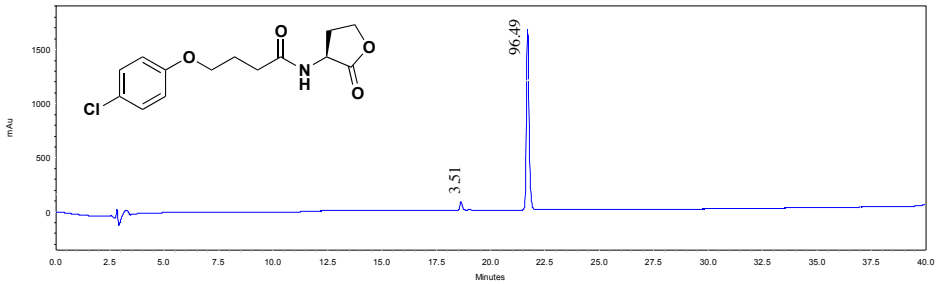

11: ESI-MS calculated m/z $[M+NH_4]^+$ 372.1952, observed m/z $[M+NH_4]^+$ 372.1949

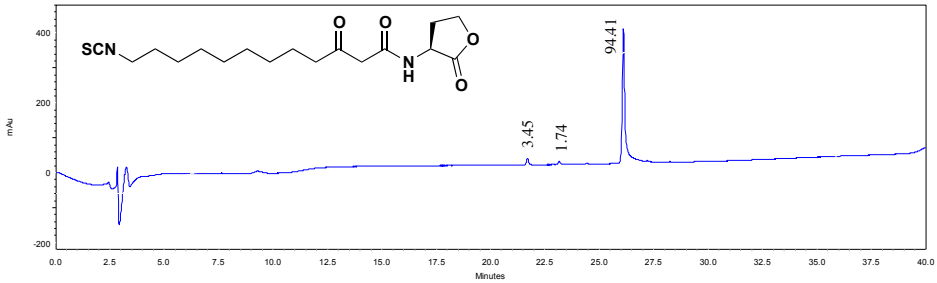

13: ESI-MS calculated m/z $[M+1]^+$ 320.2226, observed m/z $[M+1]^+$ 320.2212

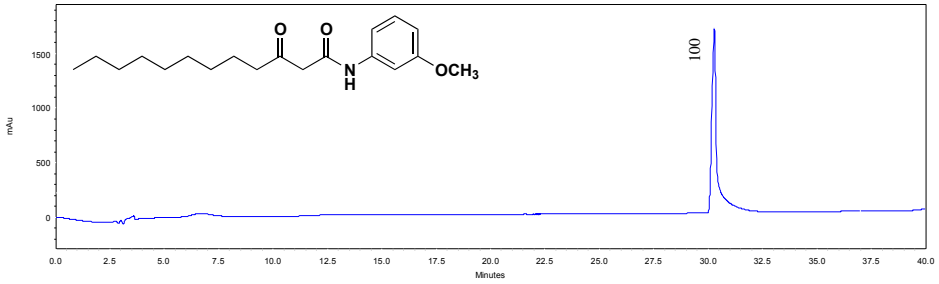

15: ESI-MS calculated m/z $[M+1]^+$ 310.2377, observed m/z $[M+1]^+$ 310.2371

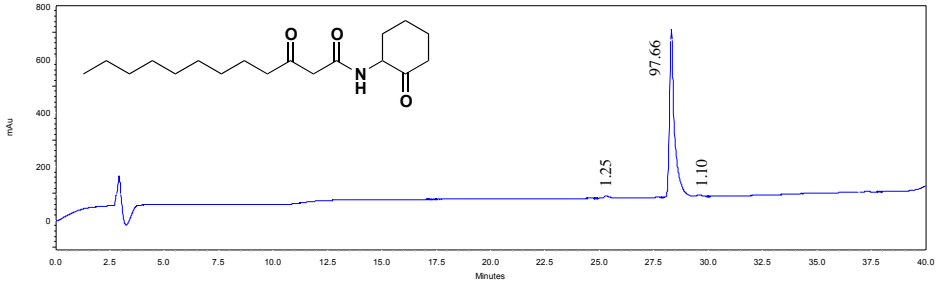

16: ESI-MS calculated m/z $[M+1]^+$ 358.0107, observed m/z $[M+1]^+$ 358.0102

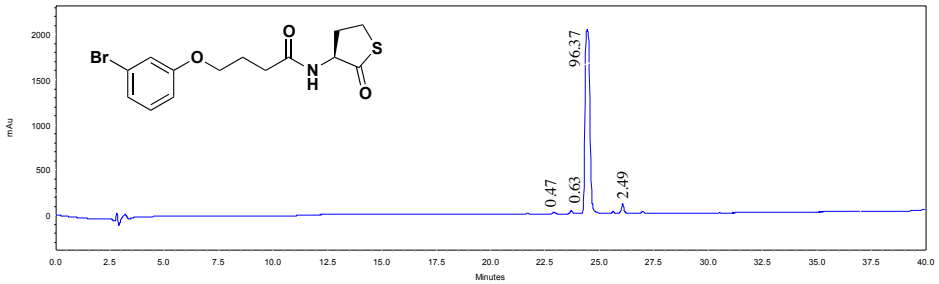

17: ESI-MS calculated m/z $[M+1]^+$ 240.2322, observed m/z $[M+1]^+$ 240.2319

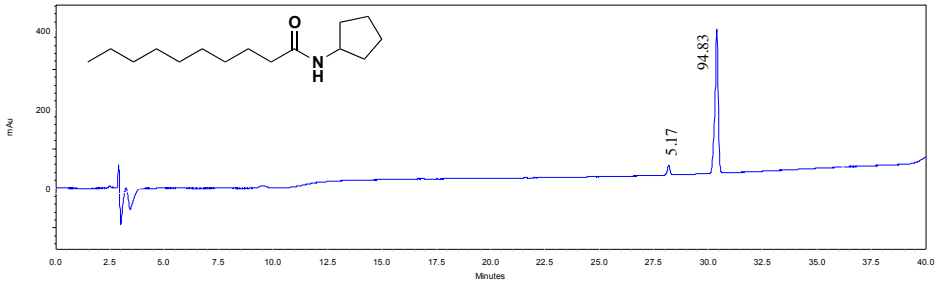

18: ESI-MS calculated m/z $[M+1]^+$ 290.2115, observed m/z $[M+1]^+$ 290.2109

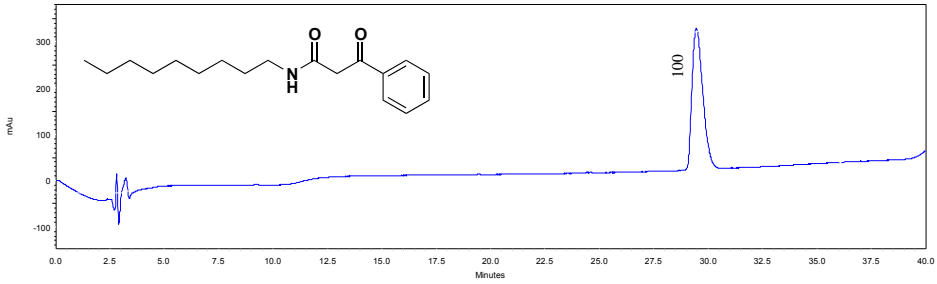

19: ESI-MS calculated m/z $[M+1]^+$ 566.8953, observed m/z $[M+1]^+$ 566.8946

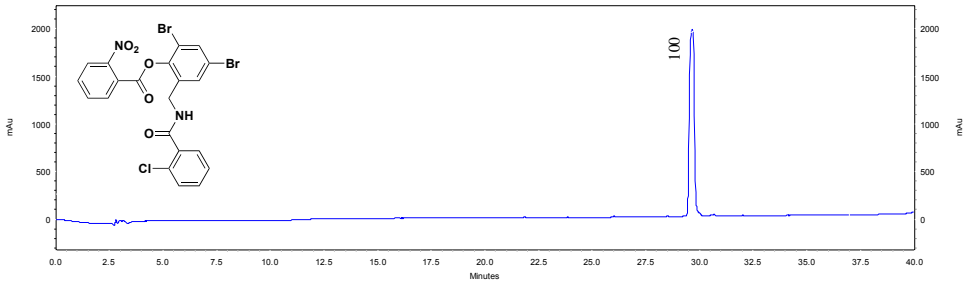

20: ESI-MS calculated m/z $[M+1]^+$ 385.0505, observed m/z $[M+1]^+$ 385.0495

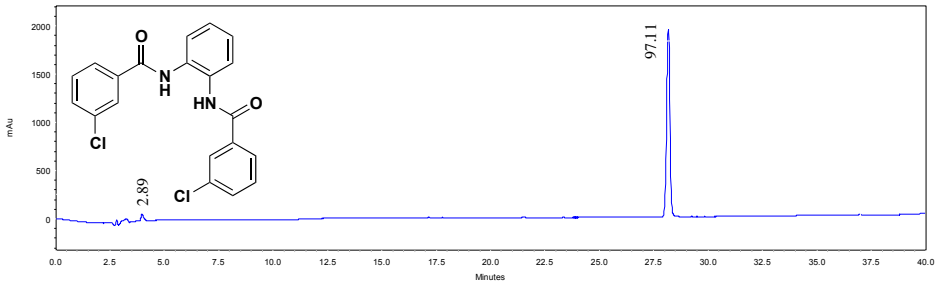

21: ESI-MS calculated m/z $[M+1]^+$ 252.8495 , observed m/z $[M+1]^+$ 252.8496

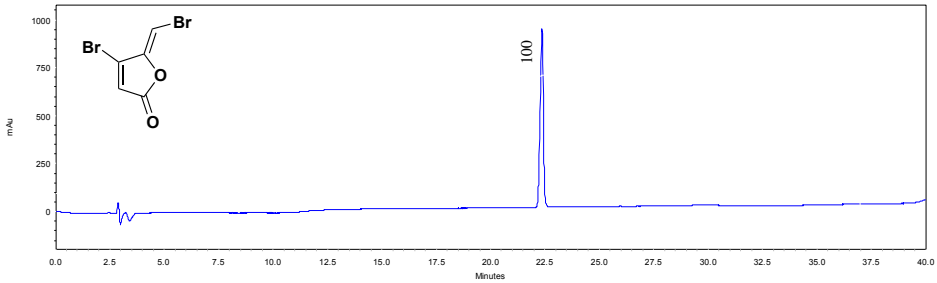

22: ESI-MS calculated m/z $[M+1]^+$ 297.2291, observed m/z $[M+1]^+$ 297.2280

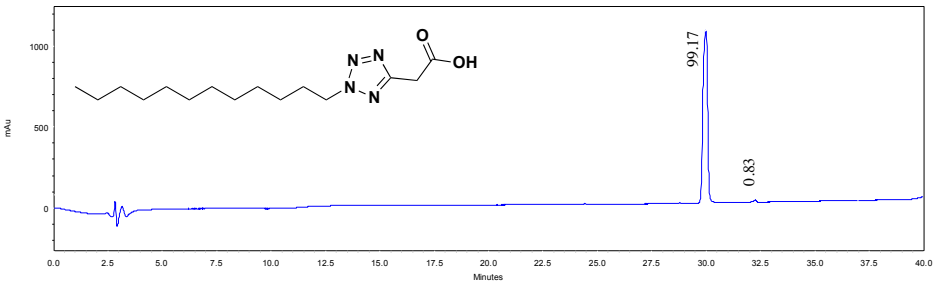

NMR Spectra.

NMR data are provided for compounds that were reported by other laboratories but synthesized in our laboratory (**10**, **13**, **16–20**, and **22**). Note, we also synthesized **19** (TP-1P) and analyzed its NMR spectra to confirm the sample provided by the Greenberg laboratory was the TP-1P isomer; these spectra for **19** are provided below.

NMR instrumentation. NMR spectra were recorded at room temperature in deuterated NMR solvents at 400 MHz on a Bruker Avance-400 with SmartProbe and SampleJet or at 500 MHz on a Bruker Avance-500 with DCH cryoprobe and SampleXpress. The purchase of the Bruker Avance-400 spectrometer by the UW–Madison Department of Chemistry was partially funded by NSF Award CHE-1048642.

1H, CDCl3, 400.18 MHz — D1504221050_Ctrl8_H.10.fid

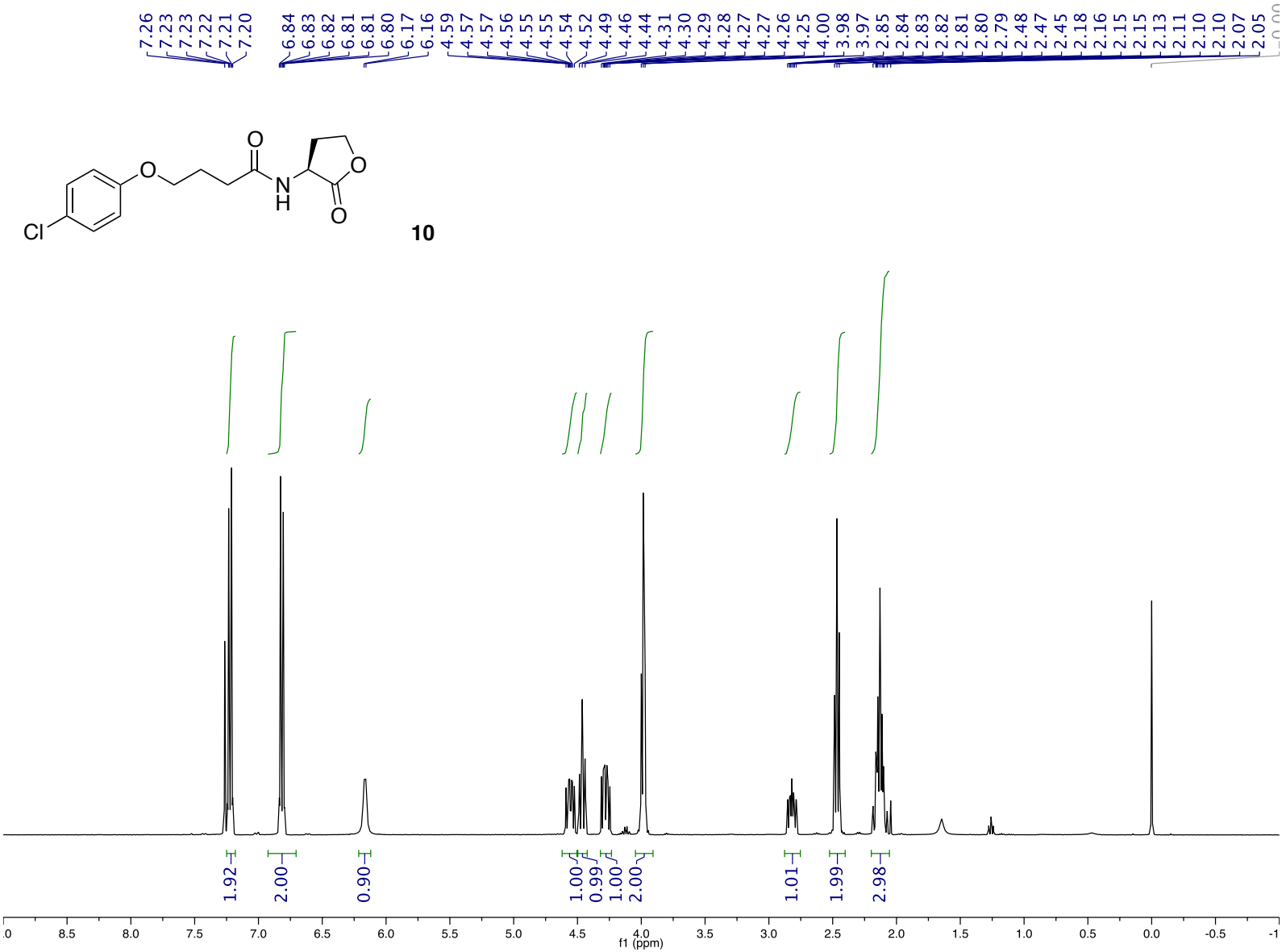

10

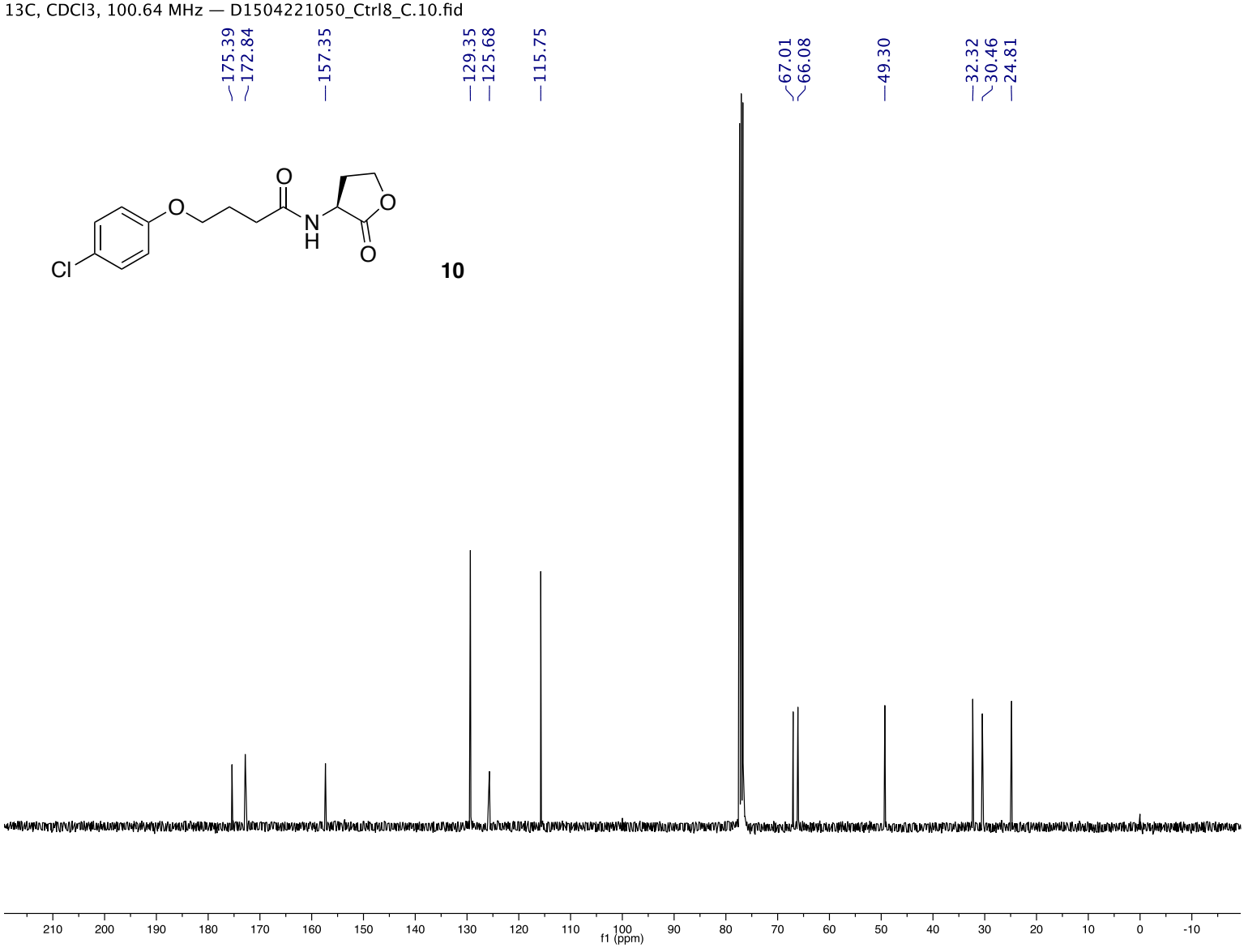
13C, CDCl3, 100.64 MHz — D1504221050_Ctrl8_C.10.fid
175.39
172.84
157.35
129.35
125.68
115.75
67.01
66.08
49.30
32.32
30.46
24.81
O
O
N
H
O
O
Cl
10
210
200
190
180
170
160
150
140
130
120
110
100
90
80
70
60
50
40
30
20
10
0
-10
f1 (ppm)

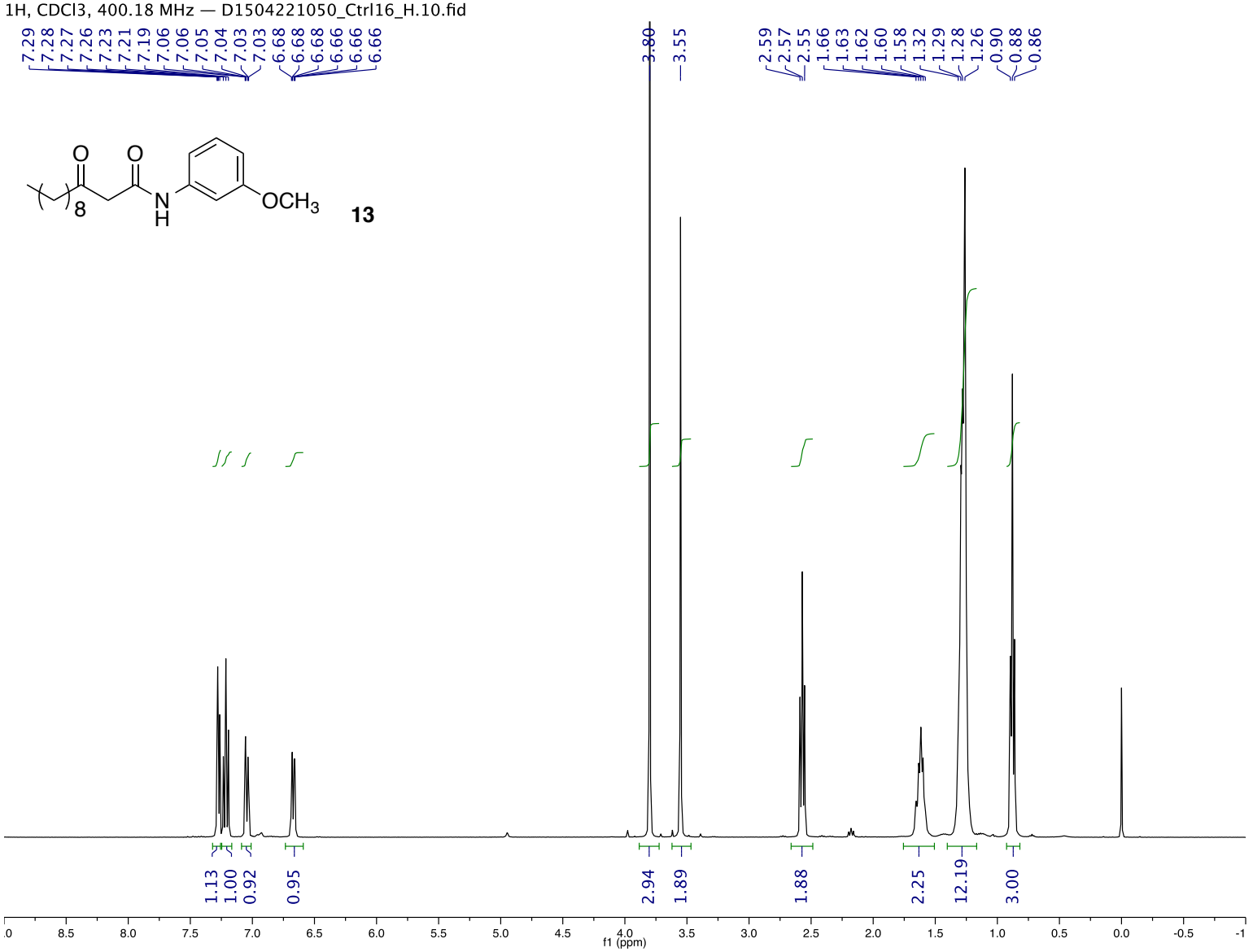
1H, CDCl3, 400.18 MHz — D1504221050_Ctrl16_H.10.fid
7.29
7.28
7.27
7.26
7.23
7.21
7.19
7.06
7.06
7.05
7.04
7.03
7.03
6.68
6.68
6.68
6.66
6.66
6.66
3.80
3.55
2.59
2.57
2.55
1.66
1.63
1.62
1.60
1.58
1.32
1.29
1.28
1.26
0.90
0.88
0.86
O
O
N
H
8
OCH3
13
1.13
1.00
0.92
0.95
2.94
1.89
1.88
2.25
12.19
3.00
f1 (ppm)

13C, CDCl3, 100.64 MHz — D1504221050_Ctrl16_H.11.fid

207.98
163.47
160.11
138.73
129.67
112.27
110.42
105.72
77.35
77.04
76.72
55.32
48.90
44.25
31.85
29.39
29.35
29.25
28.99
23.37
22.67
14.12
0.01

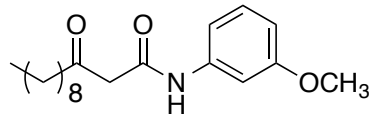

13

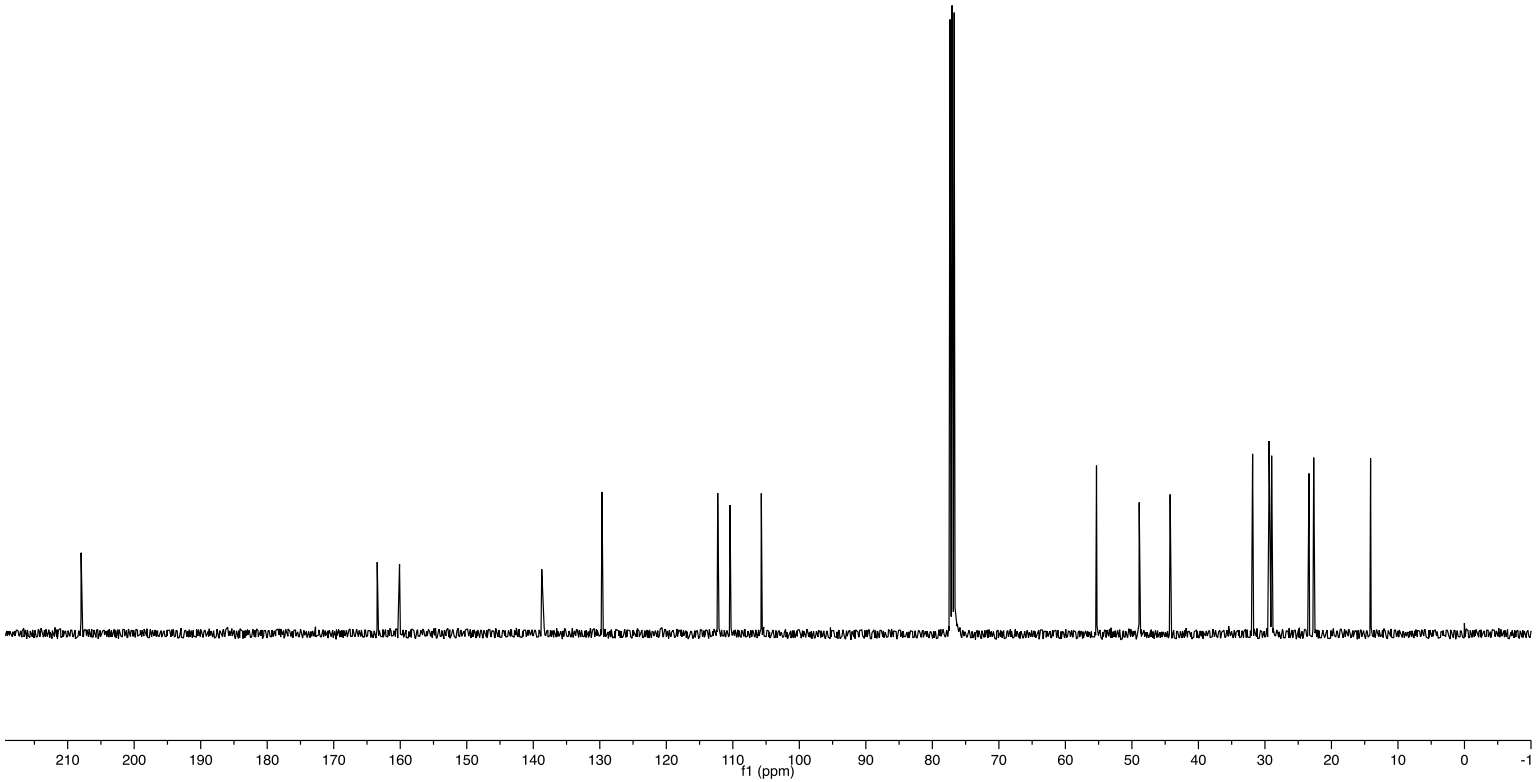

1H, CDCl3, 400.18 MHz
D1504271445_mBTL_H.10.fid

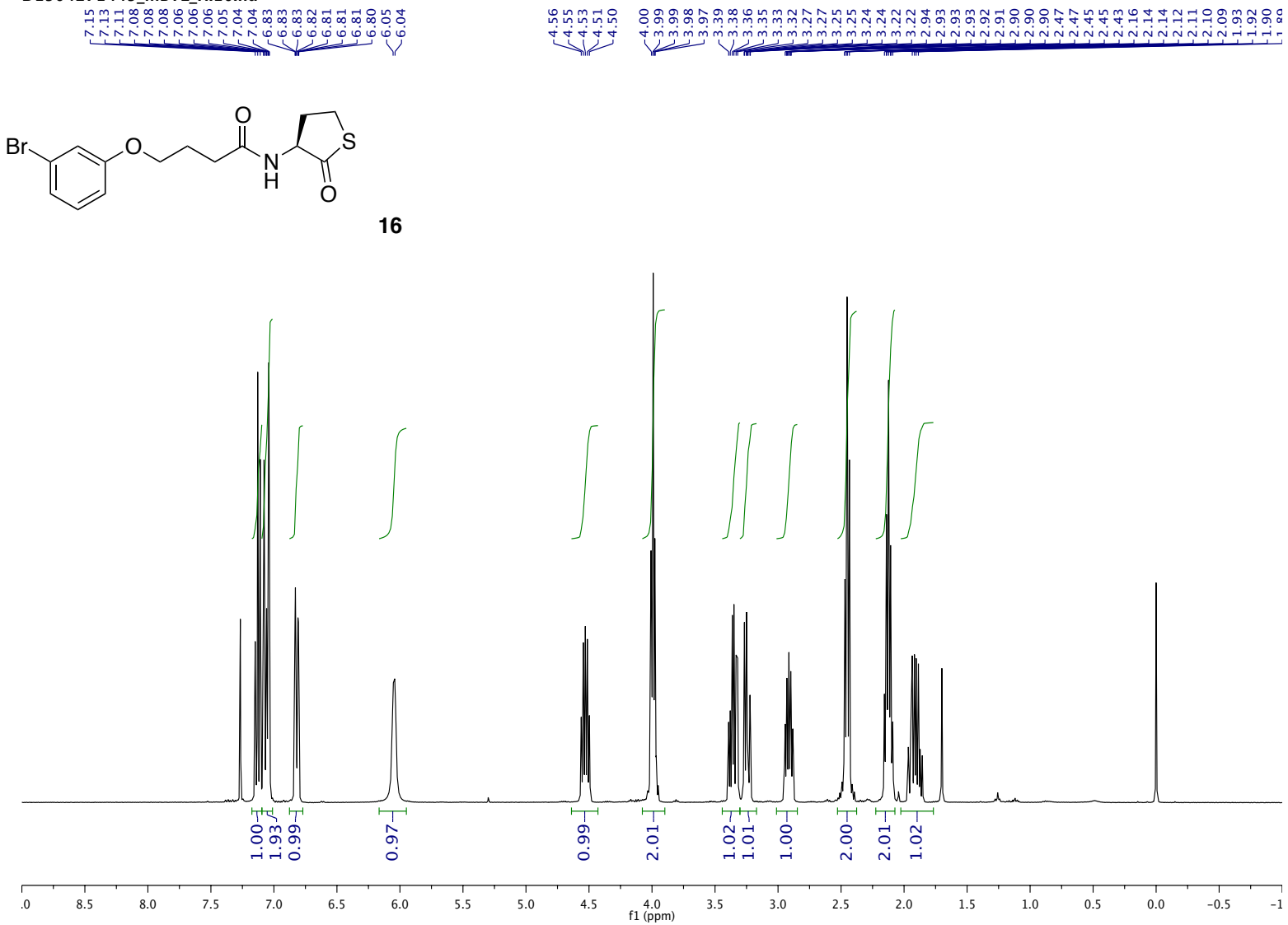

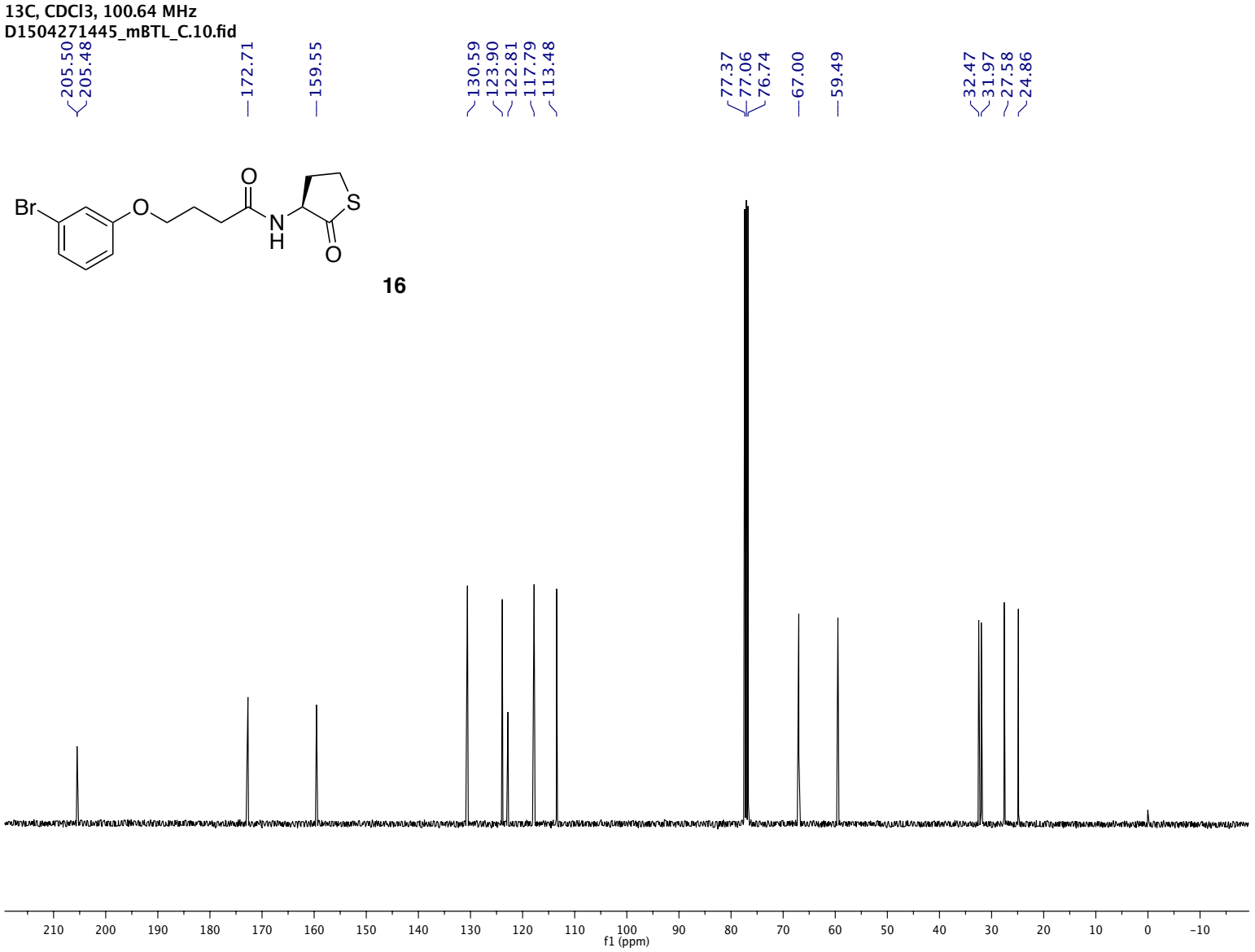
13C, CDCl3, 100.64 MHz
D1504271445_mBTL_C.10.fid
205.50
205.48
172.71
159.55
130.59
123.90
122.81
117.79
113.48
77.37
77.06
76.74
67.00
59.49
32.47
31.97
27.58
24.86
Br
O
O
N
H
S
O
16
f1 (ppm)

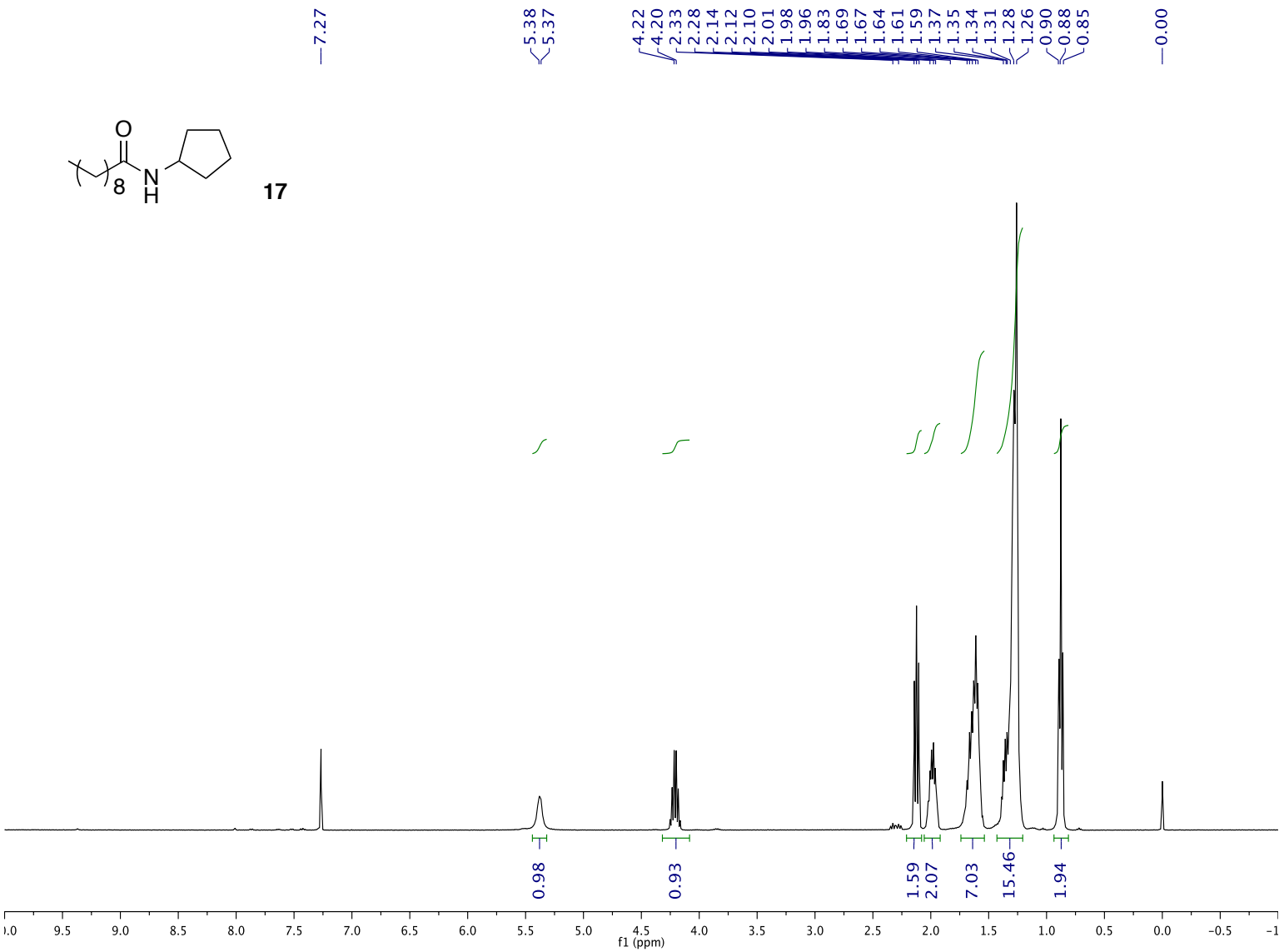
1H, CDCl3, 400.18 MHz — D1403040917_FMR28b.10.fid
7.27
5.38
5.37
4.22
4.20
2.33
2.28
2.14
2.12
2.10
2.01
1.98
1.96
1.83
1.69
1.67
1.64
1.61
1.59
1.37
1.35
1.34
1.31
1.28
1.26
0.90
0.88
0.85
0.00
O
N
H
8
17
0.98
0.93
1.59
2.07
7.03
15.46
1.94
f1 (ppm)

13C, CDCl3, 100.64 MHz — D1402141540_FMR_26b.11.fid

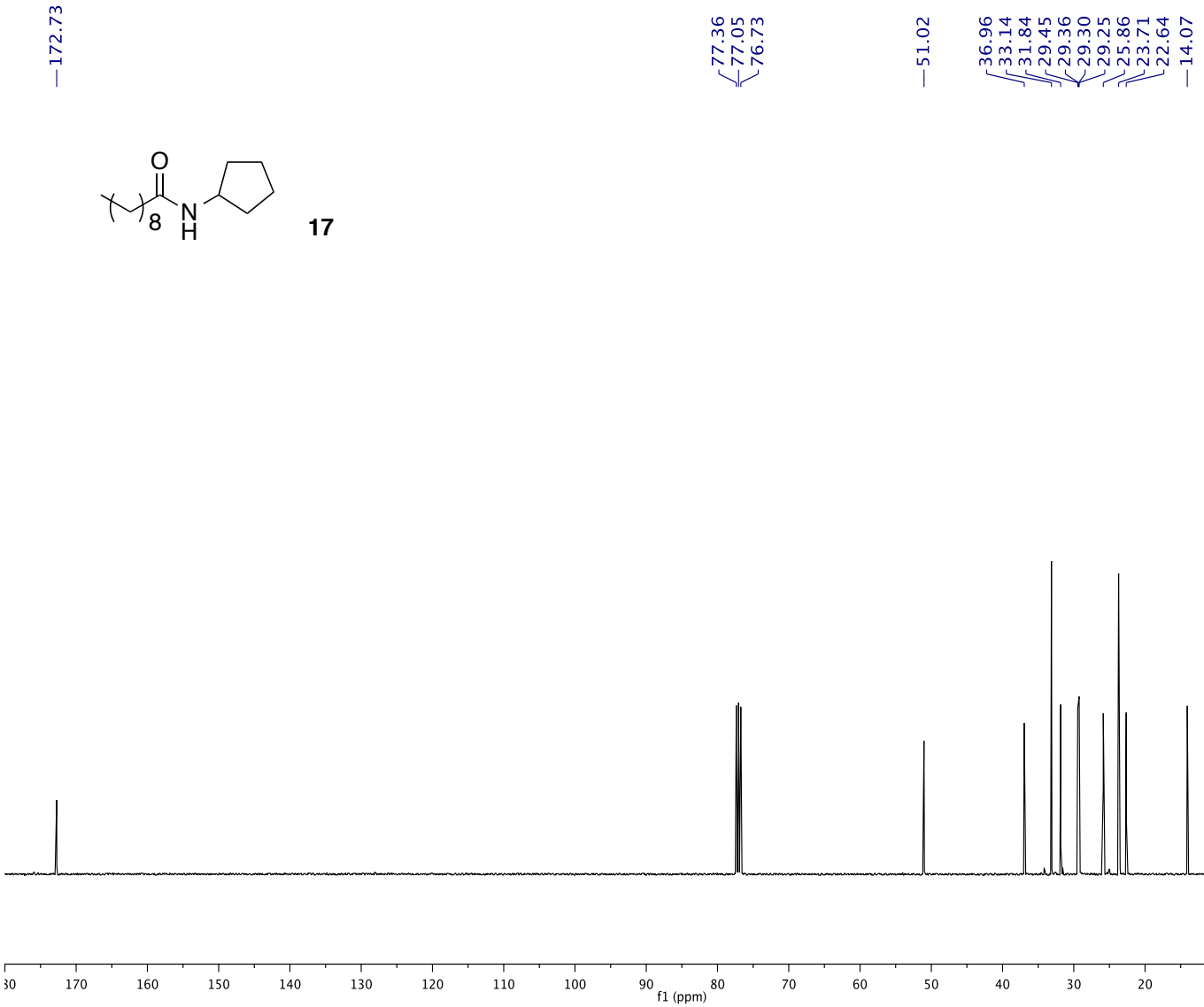

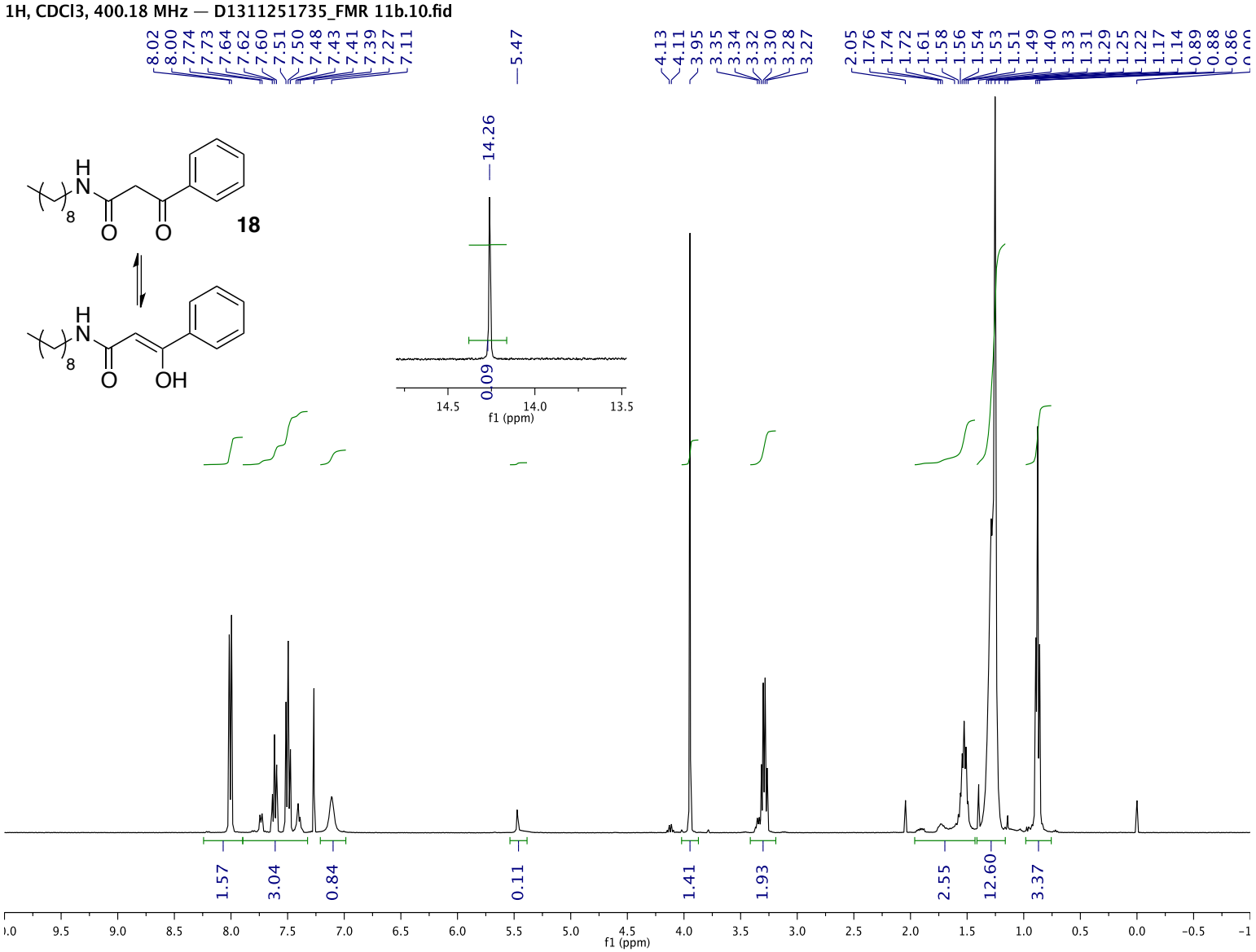
1H, CDCl3, 400.18 MHz — D1311251735_FMR 11b.10.fid
18
f1 (ppm)

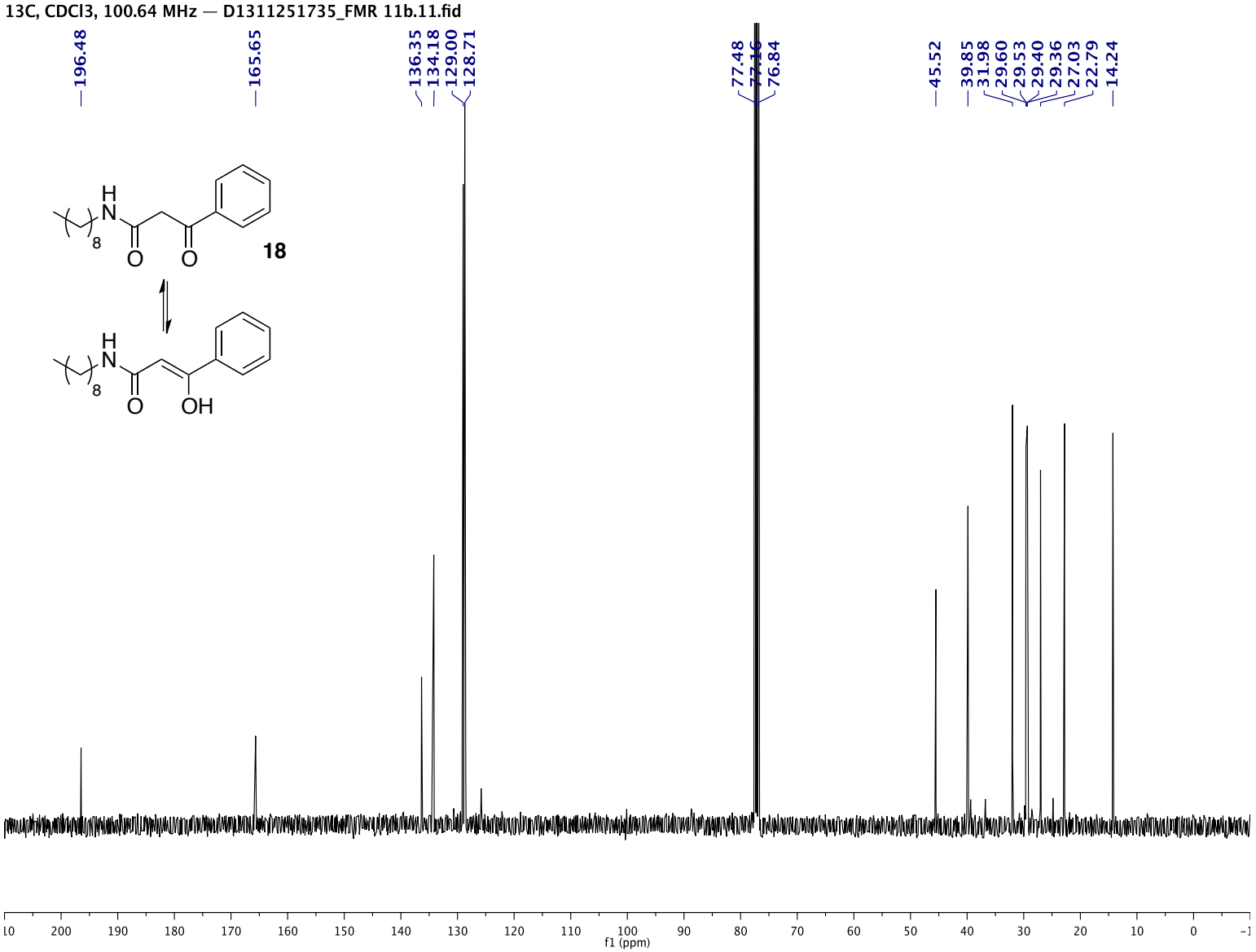
13C, CDCl3, 100.64 MHz — D1311251735_FMR 11b.11.fid
196.48
165.65
136.35
134.18
129.00
128.71
77.48
77.16
76.84
45.52
39.85
31.98
29.60
29.53
29.40
29.36
27.03
22.79
14.24
18
f1 (ppm)

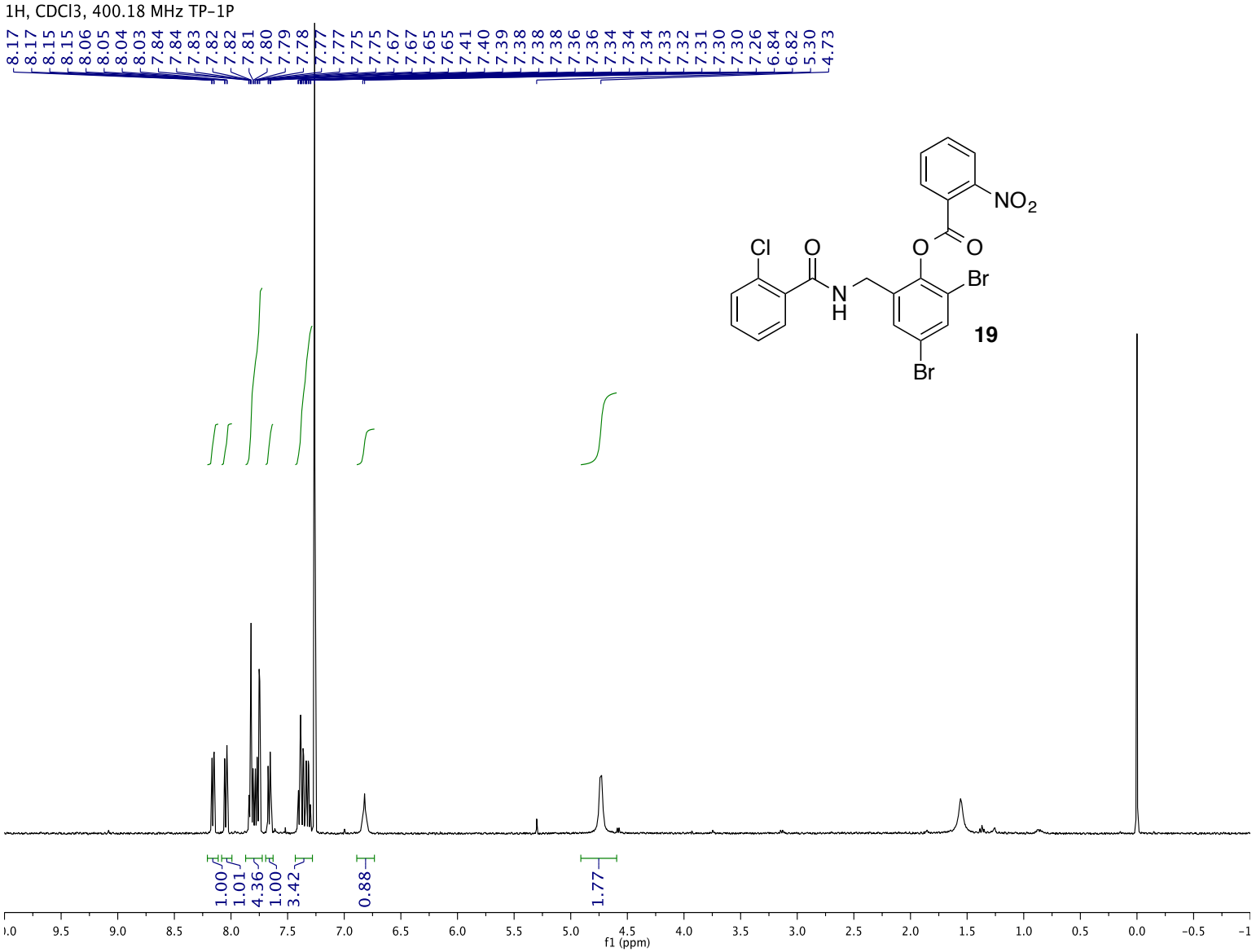
1H, CDCl3, 400.18 MHz TP-1P
8.17 8.17 8.15 8.15 8.06 8.05 8.04 8.03 7.84 7.84 7.83 7.82 7.82 7.81 7.80 7.79 7.78 7.77 7.77 7.75 7.75 7.67 7.67 7.65 7.65 7.41 7.40 7.39 7.38 7.38 7.38 7.36 7.36 7.34 7.34 7.34 7.33 7.32 7.31 7.30 7.30 7.26 6.84 6.82 5.30 4.73
NO2
Cl
O
O
O
Br
N
H
19
Br
1.00 1.01 4.36 1.00 3.42 0.88 1.77
f1 (ppm)

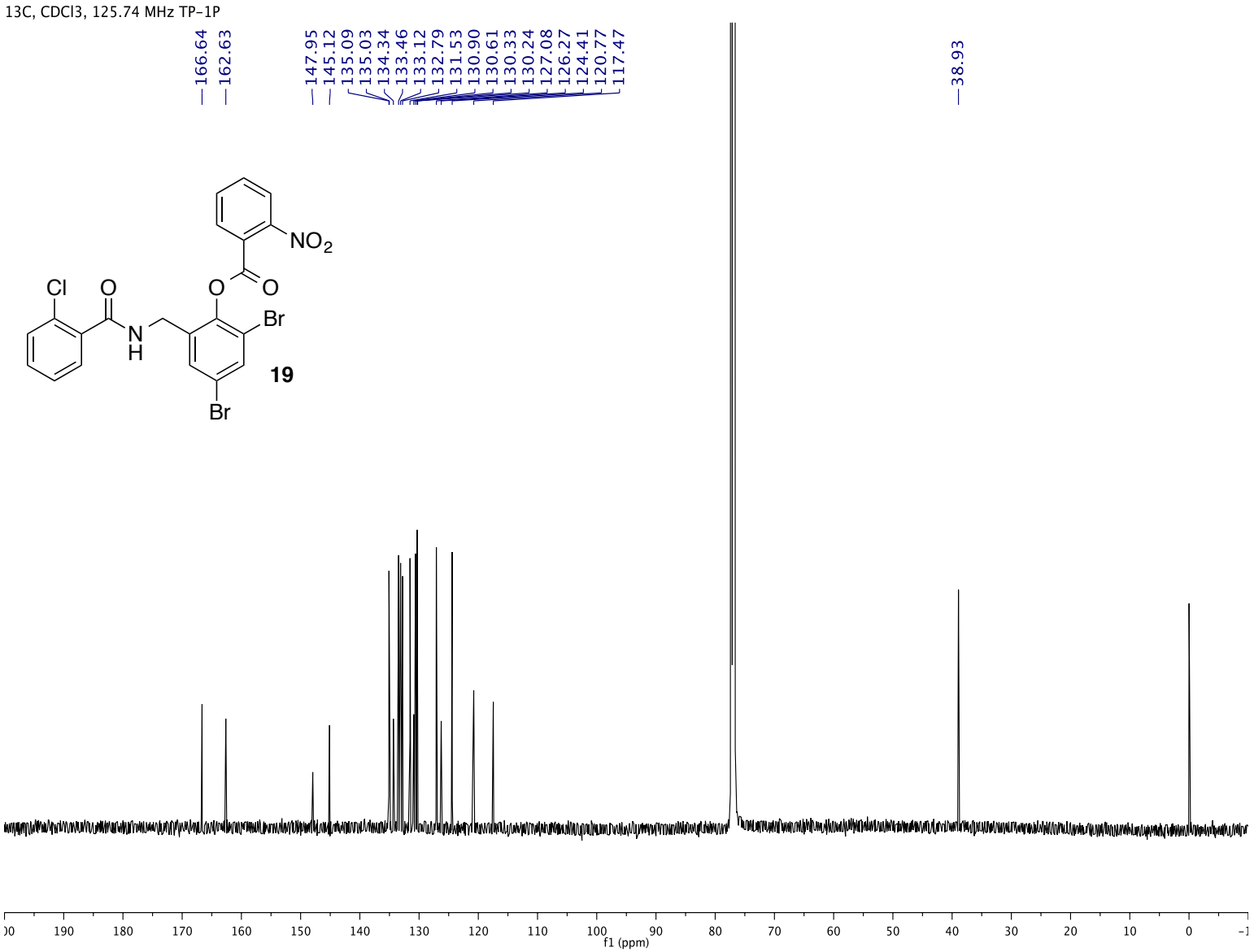
13C, CDCl3, 125.74 MHz TP-1P
166.64
162.63
147.95
145.12
135.09
135.03
134.34
133.46
133.12
132.79
131.53
130.90
130.61
130.33
130.24
127.08
126.27
124.41
120.77
117.47
38.93
NO2
Cl
O
O
O
Br
N
H
19
Br
f1 (ppm)

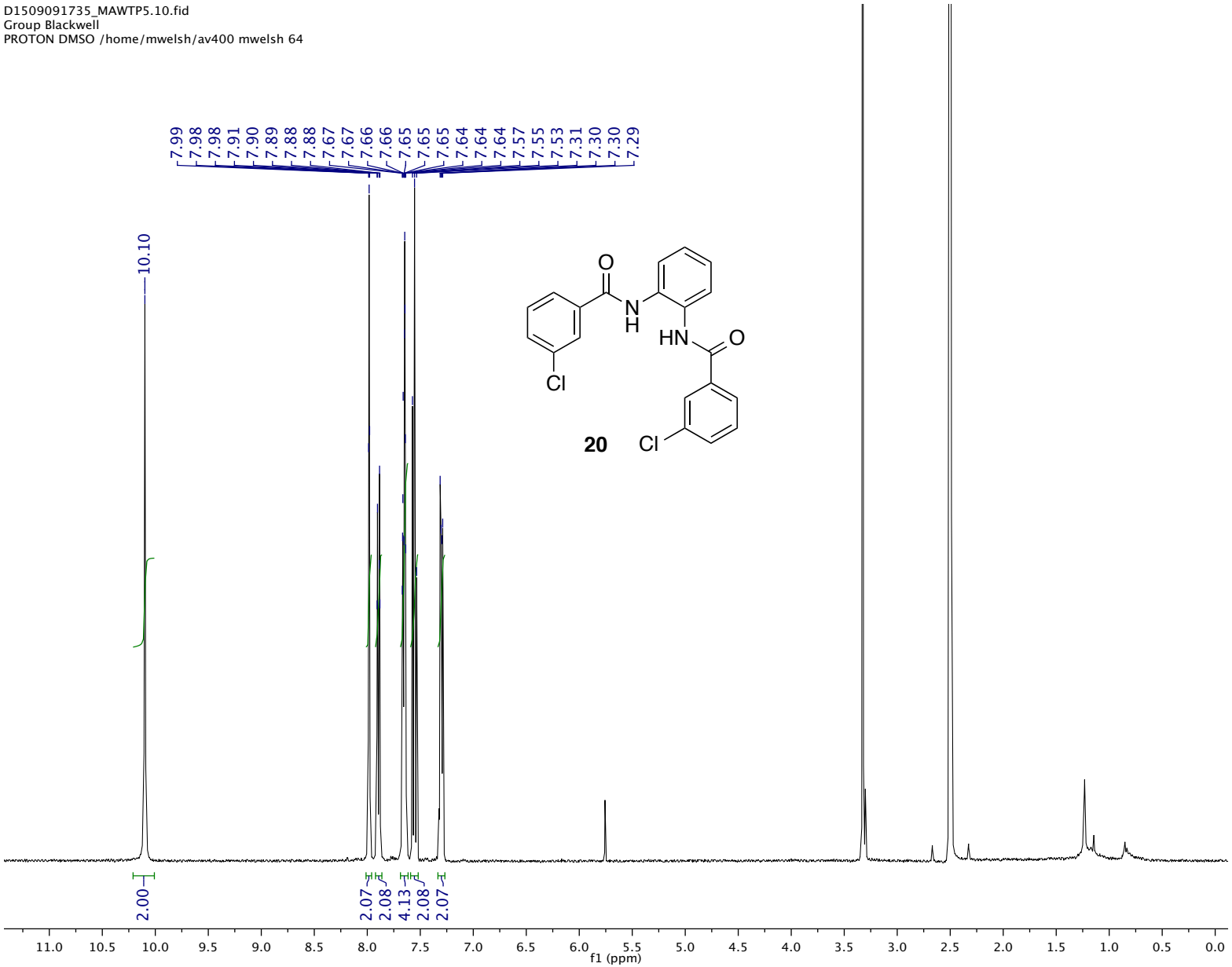
D1509091735_MAWTP5.10.fid
Group Blackwell
PROTON DMSO /home/mwelsh/av400 mwelsh 64
7.99
7.98
7.98
7.91
7.90
7.89
7.88
7.88
7.67
7.67
7.66
7.66
7.65
7.65
7.65
7.64
7.64
7.64
7.57
7.55
7.53
7.31
7.30
7.30
7.29
10.10
O
N
H
HN
O
Cl
Cl
20
2.00
2.07
2.08
4.13
2.08
2.07
11.0
10.5
10.0
9.5
9.0
8.5
8.0
7.5
7.0
6.5
6.0
5.5
5.0
4.5
4.0
3.5
3.0
2.5
2.0
1.5
1.0
0.5
0.0
f1 (ppm)

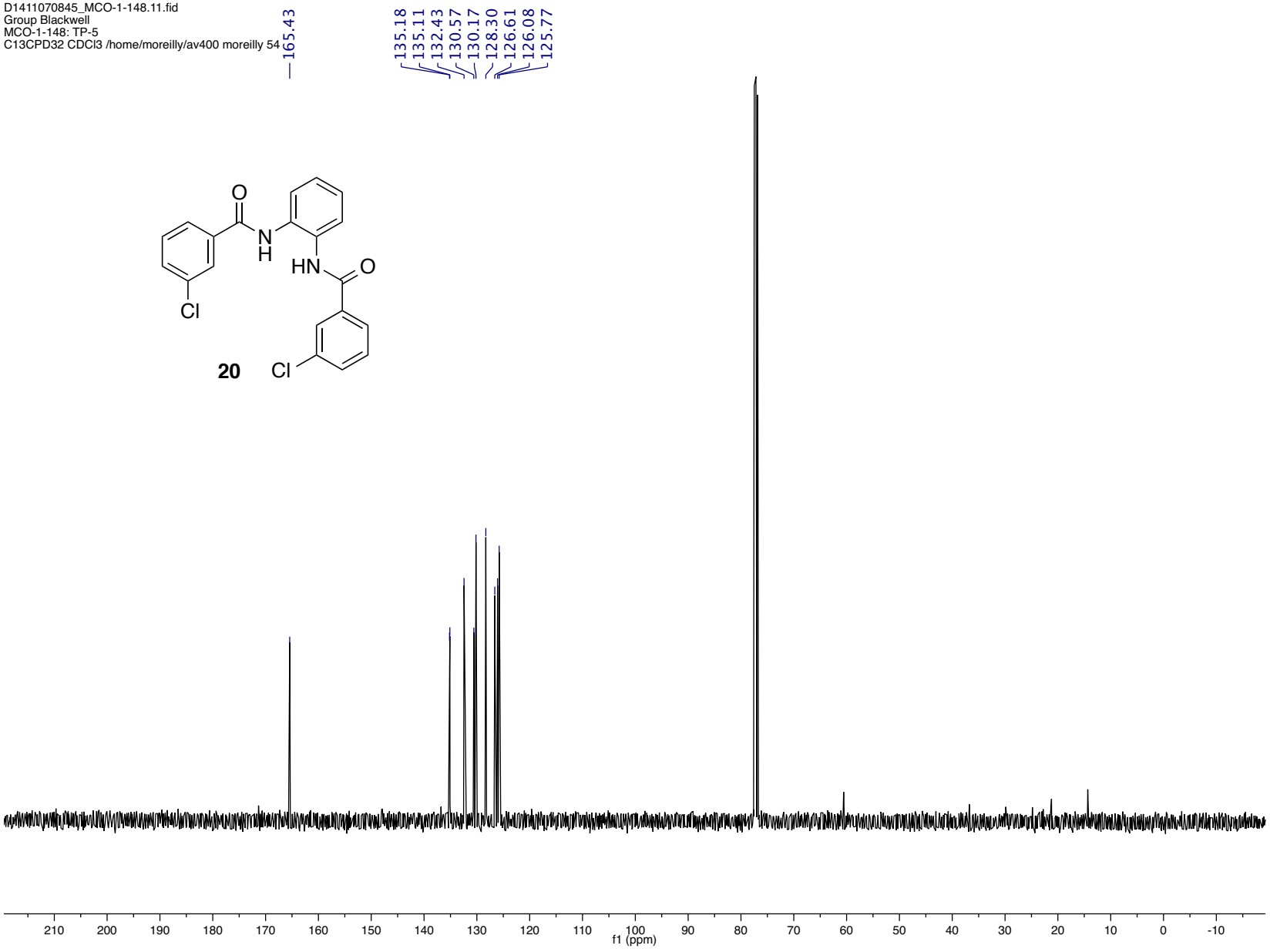
D1411070845_MCO-1-148.11.fid
Group Blackwell
MCO-1-148: TP-5
C13CPD32 CDCl3 /home/moreilly/av400 moreilly 54
165.43
135.18
135.11
132.43
130.57
130.17
128.30
126.61
126.08
125.77
O
N
H
HN
O
Cl
Cl
20
210
200
190
180
170
160
150
140
130
120
110
100
90
80
70
60
50
40
30
20
10
0
-10
f1 (ppm)

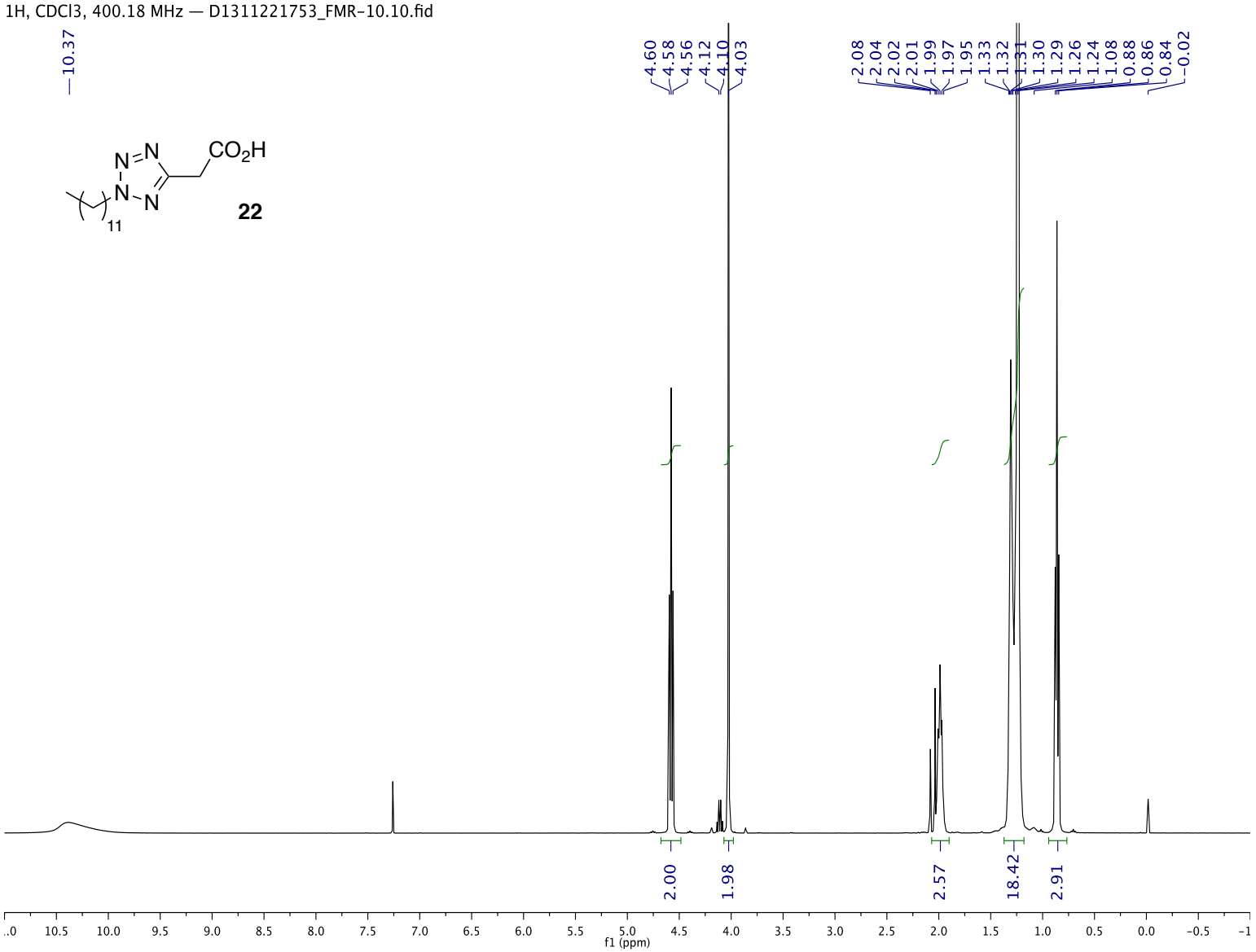
1H, CDCl3, 400.18 MHz — D1311221753_FMR-10.10.fid
10.37
4.60
4.58
4.56
4.12
4.10
4.03
2.08
2.04
2.02
2.01
1.99
1.97
1.95
1.33
1.32
1.31
1.30
1.29
1.26
1.24
1.08
0.88
0.86
0.84
0.02
CO2H
N
N
N
N
11
22
2.00
1.98
2.57
18.42
2.91
f1 (ppm)

13C, CDCl3, 100.64 MHz — D1311221753_FMR-10.11.fid

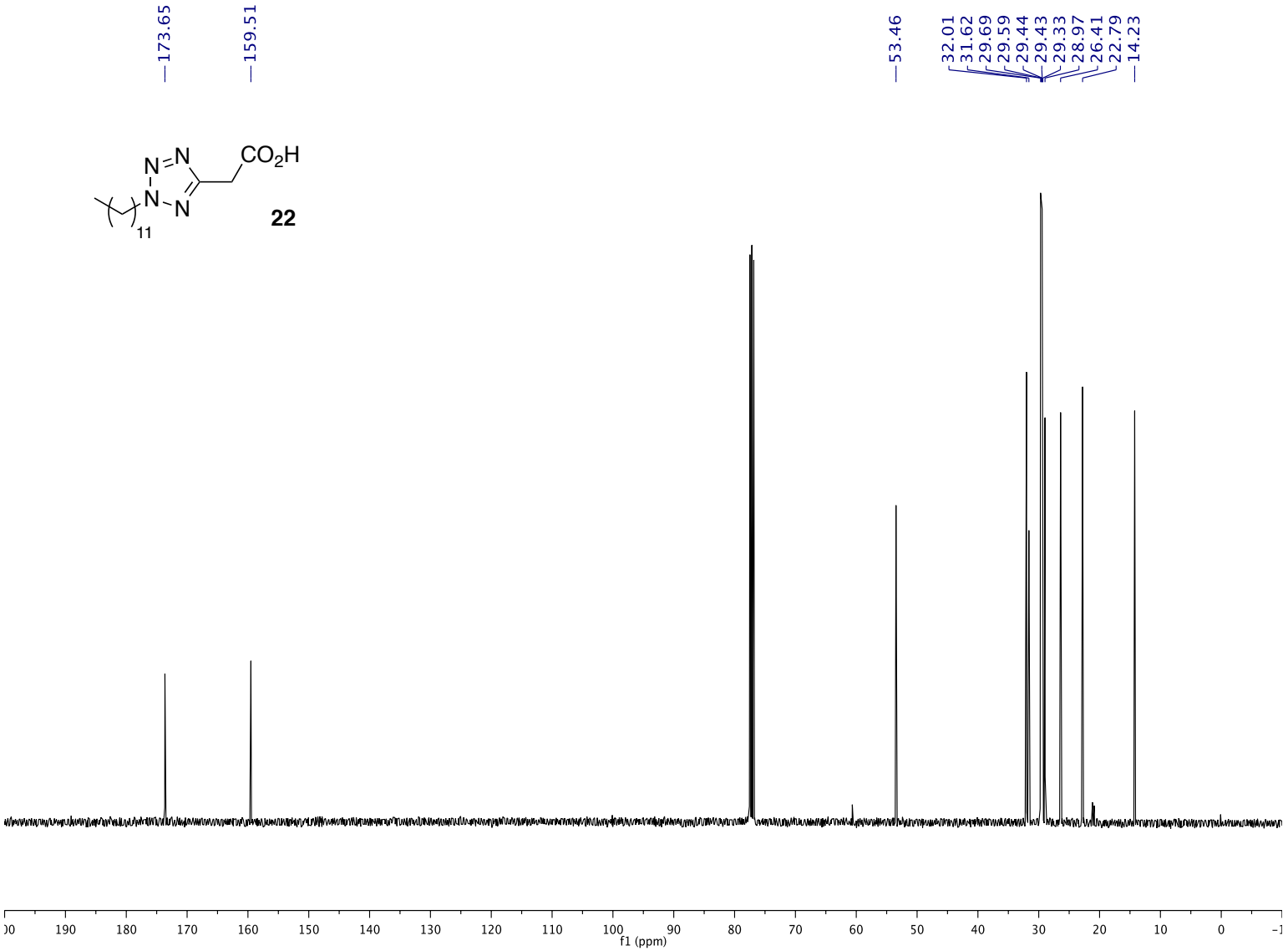

22